2014

THERAPEUTIC EFFICACY OF COMBINATION OF MTOR INHIBITORS AND AMPK ACTIVATORS IN NON-SMALL CELL LUNG CANCER.

Grinal Corriea
Virginia Commonwealth University

THERAPEUTIC EFFICACY OF COMBINATION OF MTOR INHIBITORS AND AMPK ACTIVATORS IN NON-SMALL CELL LUNG CANCER.

A thesis submitted in partial fulfillment of the requirements for the degree of Master of Science at Virginia Commonwealth University.

By

Grinal Michael Corriea

Bachelor of Pharmacy, University of Mumbai, 2010

Advisor: Richard G. Moran, PhD

Professor, Department of Pharmacology & Toxicology

Virginia Commonwealth University

Richmond, Virginia

July 2014

To my beloved Parents,

Mr. Michael Corriea and Mrs. Rosemary Corriea.

The reason why I exist.

ACKNOWLEDGEMENTS

I would like to express my sincere gratitude to all those who have supported me and contributed towards my graduate studies both, personally and professionally. First, I would like to thank my advisor, Dr. Richard Moran, for his guidance, time, and having faith in me. I would like to specially thank him for being very patient with me and continuously supporting me. The education and experience I have obtained from his laboratory has made me a critical thinker and has laid a strong foundation for my career. I would also like to thank my committee members, Dr. Shirley Taylor and Dr. Hamid Akbarali, for their constant encouragement and motivation. I greatly appreciate the time they have invested in my graduate studies and advising me from time to time.

I would also like to thank my lab members, Dr. Chen Yang, Charles Lyons, and especially Stuti Agarwal and Catherine Bell and for constantly providing me with scientific insights and being there for me. I will always cherish the friendship I have developed with them. I wish them each all the best success in their own careers. I would like to thank Taylor lab members, Dr. Timothy Lochmann, Elliot Burton, John Strang, Shannon Hedricks, and Dr. Prashant Thakkar for their advice and encouragement throughout the course of this thesis.

I would like to thank the Department of Pharmacology and Toxicology for accepting me into this program and giving me an opportunity to showcase my caliber.

I must thank my wonderful family without which I would not be able to purse my graduate studies. I am immensely blessed to have Michael Corriea and Rosemary Corriea as my parents. They have always believed in me and I am sure they are proud of this achievement of mine. I must also thank my to-be parents Felix Pereira and Smita Pereira for always being there for me. I am indeed lucky to have two loving set of parents who have remained by my side through thick and thin.

I would also like to thank my awesome fiancé Warren Pereira for loving me so much and always supporting me. This journey of my graduate studies would not be complete without his constant faith in me. I am extremely grateful to him for coming into my life and making me a better person, both personally and professionally.

Last but not the least; I am thankful to the Almighty for keeping me safe and sound throughout my graduate studies.

Table of Contents

LIST OF TABLES

LIST OF FIGURES

LIST OF ABBREVIATIONS

μmol/L – Micromoles per liter

4E-BP1 - Eukaryotic initiation factor 4E binding protein

Ab - Antibody

AICAR - Aminoimidazolecarboxamide ribonucleoside

AICART - Aminoimidazolecarboxamide ribonucleotide formyltransferase

AMP – Adenosine monophosphate

AMPK - AMP-activated protein kinase

ATP – Adenosine triphosphate

CAMKKβ - Calmodulin-dependent protein kinase kinase β

CDK4/6 – Cyclin dependent kinases 4/6

CDKN2A - Cyclin-dependent kinase inhibitor 2A

CI – Combination index

DDR2 - Discoidin domain-containing receptor 2

Deptor - DEP-domain-containing mTOR-interacting protein

dFBS – Dialyzed fetal bovine serum

DMSO - Dimethyl sulfoxide

DNA - Deoxyribonucleic acid

EDTA - Ethylenediaminetetraacetic acid

EGFR – Epidermal growth factor receptor

EGTA - Ethylene glycol tetraacetic acid

eIF4E - Eukaryotic initiation factor 4E

Fa - Affected fraction

FBS – Fetal bovine serum

FGFR - Fibroblast growth factor receptors

FKBP12 - FK506-binding protein of 12 kD

FoxO1/3a - Forkhead Box O1/3a

FRB - FKBP12- rapamycin binding domain

g - Gram

G6Pase - Glucose-6-phosphatase

GLUT4 - Glucose transporter 4

GTP - Guanosine triphosphate

HER2 - Human epidermal growth factor receptor 2

IARC - International Agency for Research on Cancer

IC50- 50% inhibitory concentrations

IGF-I - Insulin-like growth factor 1

IGF-IR - Insulin-like growth factor-I receptor

IGFR-1- Insulin-like growth factor 1 receptor

IP - Immunoprecipitation

IRS1 – Insulin receptor substrate 1

KRAS - Kirsten rat sarcoma

LKB1 - Liver kinase B1

m7GTP – 7-methyl guanosine triphosphate

MAP - Mitogen-activated protein

MAPK – Mitogen activated protein kinase

MEK - Mitogen/extracellular signal-regulated kinase

mg - Milligram

ml - Milliliter

mLST8 - Mammalian lethal with Sec13 protein 8

mm - millimeter

mM - Millimolar

mRNA – Messenger ribonucleic acid

mSIN1 - Mammalian stress-activated MAP-kinase interacting protein

mTOR - Mammalian target of rapamycin

mTORC1 - mTOR complex 1

mTORC2 - mTOR complex 2

NaF – Sodium fluoride

ND – No Drug

nm - Nanometre

nM - Nanomolar

NP40 – Nonidet P40

NSCLC - Non-small cell lung cancer

PBS - Phosphate buffered saline

PDGFR – Platelet derived growth factor receptor

PDK1 - Phosphoinositide-dependent protein kinase-1

PEPCK - Phosphoenolpyruvate carboxykinase

PH – pleckstrin homology

PI3K - Phosphoinositide 3-kinase

PIP2 - Phosphatidylinositol 4,5-bisphosphate

PIP3 - Phosphatidylinositol (3,4,5)-trisphosphate

PKB/Akt - Phosphoinositide-3-kinase-family member kinase B/Akt

PKCα - Protein kinase Cα

PRAS40 - Proline rich Akt substrate 40

Protor-1/2 - Protein observed with Rictor 1 and 2

PTEN - Phosphatase and tensin homolog

PTX – Pemetrexed

PVDF - Polyvinylidene difluoride

Rheb- Ras homolog enriched in brain

Rictor - Rapamycin-insensitive companion of mTOR

Rpm – Revolutions per minute

RPMI – Roswell park memorial institute

RSK1 - Ribosomal S6 kinase 90 kD, polypeptide 1

RTK – receptor tyrosine kinase

S6K1 – S6 Kinase 1

SD – Standard deviation

SDS - Sodium dodecyl sulfate

SGK1 - Serum/glucocorticoid-regulated kinase 1

STK11 - Serine/threonine kinase 11

TBS-T – Tris buffered saline-tween 20

TdR - Thymidine

TKI - Tyrosine kinase inhibitors

TSC – Tuberous sclerosis

ULK1/ULK2 - UNC-51-like kinases 1/2

US FDA – United States Federal Drug Administration

VEGFR – Vascular endothelial growth factor receptor

WHO - World Health Organization

ZMP - Aminoimidazolecarboxamide ribonucleotide

μM - Micromolar

Abstract

THERAPEUTIC EFFICACY OF COMBINATION OF MTOR INHIBITORS AND AMPK ACTIVATORS IN NON-SMALL CELL LUNG CANCER.

By Grinal Michael Corriea, Master of Science.

A thesis submitted in partial fulfillment of the requirements for the degree of Master of Science at Virginia Commonwealth University.

Virginia Commonwealth University, 2014

Major Director: Richard G. Moran, PhD, Professor, Department of Pharmacology & Toxicology

Pemetrexed (PTX), an antifolate drug, has been approved by the US FDA for first line therapy of mesothelioma and non-small cell lung cancer. In addition to its primary site of action on thymidylate synthase (TS), PTX also inhibits the second folate-dependent enzyme of purine biosynthesis aminoimidazolecarboxamide ribonucleotide formyltransferase (AICART). The accumulation of the substrate for AICART, ZMP, in PTX-inhibited cancer cells leads to activation of AMP-activated protein kinase (AMPK) with subsequent inhibition of mammalian target of rapamycin (mTOR) and hypophosphorylation of its downstream targets responsible for protein synthesis and cell proliferation. Inhibitors of mTORC1 like Rapamycin and its analogs (rapalogs) have only partial effects on tumor cells as they do not inhibit mTORC2, which phosphorylates Akt subsequently relieving the inhibition of

mTORC1, thus leading to poor cytotoxicity by rapalogs. AMPK exerts control on mTORC1 kinase activity and PTX mediated activation of AMPK leads to its subsequent downregulation and hence, would be expected to have a therapeutic interaction with direct mTOR inhibitors. AZD8055, an ATP-competitive inhibitor of mTOR kinase, potently inhibits both mTORC1 and mTORC2 and therefore, can overcome the feedback mechanism(s) limiting the action of rapalogs to cytostatic effects. To study the effects of AMPK activation and mTOR inhibition pharmacologically, we performed growth suppression assays using pemetrexed, AICAR, RAD001, and AZD8055. The effect of inhibition of mTOR with these drugs was assessed by examining the dephosphorylation of mTORC1 substrates S6K1 and 4E-BP1, as single agents and in combination, at their 50% inhibitory concentrations (IC_{50}) by western blotting. Our data suggested that AMPK activation via PTX mediated AICART inhibition in combination with direct mTOR inhibition by AZD8055 has a synergistic interaction on the proliferation of NSCLC cells in culture. Inhibition of mTOR endogenously by pemetrexed, along with direct pharmacological inhibition of mTOR prevents the feedback circuit which may compromise the therapeutic efficacy of rapamycin analogs. Pemetrexed and AZD8055, as single agents, demonstrated inhibitory activity on phosphorylation events of mTORC1 substrates. This activity was markedly increased by combining both the drugs. Our findings suggest that direct inhibitors of mTOR enhance the effects of activators of AMPK. These effects appear to be mediated via combined effects on mTORC1. Taken together, the combination of catalytic site mTOR inhibitors and pemetrexed is a promising therapeutic strategy and calls for further preclinical and clinical investigations.

Chapter 1: Overview and Introduction

1.1 Cancer

The World Health Organization (WHO) reports cancer as the leading cause of death, accounting for 8.2 million deaths worldwide in 2012. (Globocan 2012, IARC). According to the American Cancer Society, cancer is the second leading cause of death in the western world, and one in 4 deaths is due to cancer (Siegel et al. 2013). Cancer arises when cells in a part of the body start to grow out of control because of mutations in genes controlling cell growth and division. Mutations and losses of the tumor suppressor genes and/or mutations or overexpression of oncogenes (see below) are the chief causes of cancer. In most cases, cancer remains undetected until the tumor has metastasized or spread to other organs in the body from its primary site. Thus, there is a need for characterizing biomarkers that can detect the early signs of cancer before the disease has progressed far and can still be treated and cured.

The management of cancer includes several approaches, including surgery, radiation, immunotherapy and chemotherapy. Chemotherapy involves a broad range of drugs that attempt to preferentially target the rapidly dividing cancer cells and cause cytotoxicity. The ultimate objective is to kill every single cancer cell in the body. Traditional cytotoxic anti-cancer drugs often target DNA synthesis or mitosis. As one would expect, these drugs can act on normal, rapidly dividing cells and lead to adverse events (Ali and Bhattacharya 2014). Recent classes of "targeted" chemotherapeutic agents bind to or downregulate a specific protein or complex involved in cancer signaling pathways and inhibit the growth of and/or induce cytotoxicity of cancer cells. Because of their specificity, they usually cause less host toxicity (Winkler et al. 2014). However, similar to other chemotherapeutics, the therapeutic efficacy of even targeted anti-cancer compounds is limited by the emergence of resistance and by toxicity profiles.

Tumors are classified as malignant or benign. Benign tumors are localized, do not spread to or invade other tissues and can often be surgically removed. They are not usually considered to be life threatening.

Malignant tumors on the other hand have the potential to invade other tissues and metastasize to distant sites. Deaths due to cancer are caused principally by metastatic disease.

1.2 Non-small cell lung cancer

Lung cancer is responsible for 26% and 28% of all female and male cancer deaths, respectively and non-small cell lung cancer (NSCLC) accounts for 80–85% of lung cancers (Siegel et al. 2013). Smoking is the main cause of lung cancer. Treatment therapies were previously based on histological classification of NSCLC; however the current paradigm for cancer treatment has shifted emphasis on targeting the mutations in the tumor that sustain the tumor phenotype ("driver mutations"). The WHO classifies NSCLC into the following subtypes: Squamous cell carcinoma (25%), Adenocarcinoma (40%) and large cell carcinoma (10%). There are several other subtypes, like neuroendocrine tumors and carcinomas with pleomorphic, sarcomatoid, or sarcomatous elements, but they are present at lower frequencies. Squamous cell carcinomas are frequently located centrally in the larger bronchi of the lung and are most frequently associated with smoking. Adenocarcinomas, on the other hand, are the most frequently studied lung cancers and are further subclassified. They are associated with heterogeneous mutations and are aggressive in nature (Brambilla et al. 2001, Heavey et al. 2014).

A tumor suppressor gene, as the name suggests, is a gene whose protein product protects a cell from progressing towards the behavior of a cancerous cell. Alteration or loss of function of these genes is harmful and can cause tumors to arise. On the other hand, an oncogene is a gene that has a potential to cause cancer; over expression or increased activation of these genes is seen in cancers (Weinberg, Robert A (2014) "The Biology of Cancer" Garland Science, page 231). It has been shown that a total of 26 genes are frequently mutated in lung adenocarcinomas, of which 10 genes including the tumor suppressor genes p53, CDKN2A and STK11; and several oncogenes like KRAS and EGFR are most frequently mutated (Ding et al. 2008). Squamous cell carcinomas also harbor mutations in the p53 gene; however, there are additional mutations in genes including, but not limited to, PI3KCA, PTEN, DDR2 and FGFR in

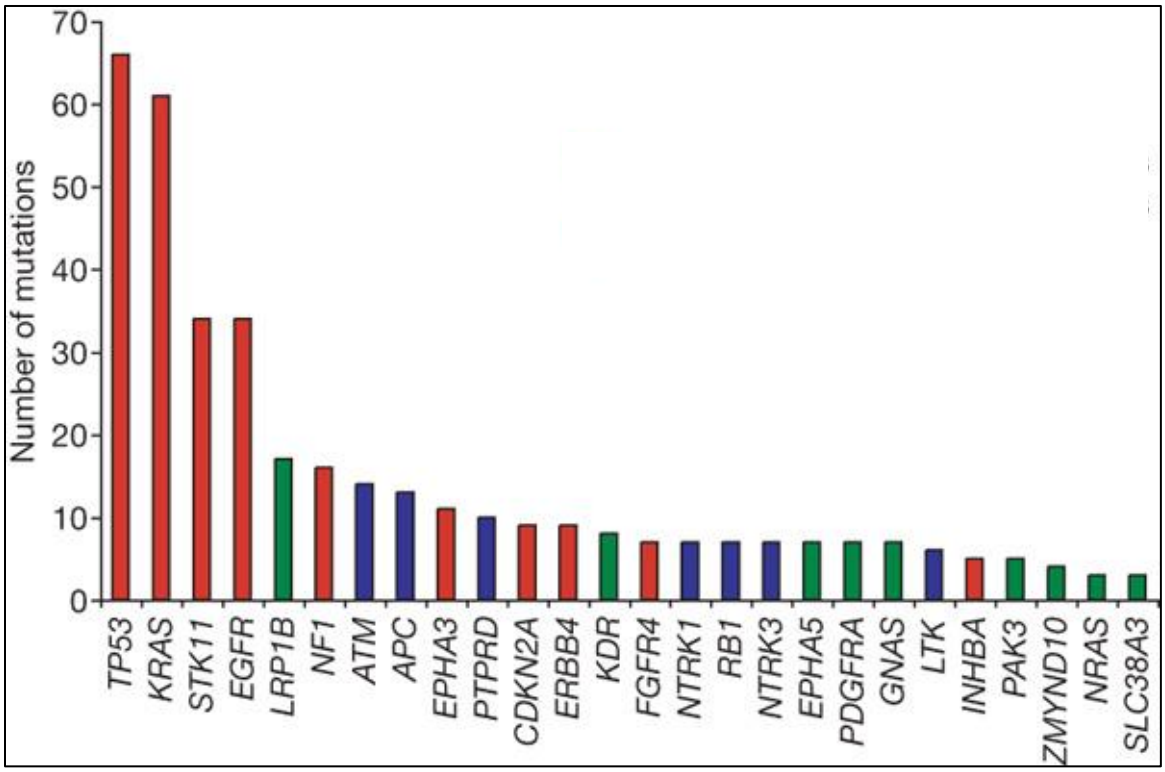

Figure 1. Most frequently mutated genes in lung adenocarcinomas

The X- axis represents the number of somatic mutations in each indicated gene (Y- axis) in 188 tumor and normal pairs. Red bars indicate that these genes were found to be significantly mutated by three statistical methods (10 genes); blue bars - at least two methods (7 genes); and green bars - one of the three methods (9 genes), for up to 26 significantly mutated genes in total. Figure adapted from Ding et al., Nature 455, 1069 – 1075 (2008)

these cancers (D'Arcangelo et al. 2013). Identification of a number of driver mutations in NSCLC and other cancers has put an emphasis on tumor biopsies and molecular characterization of tumors, laying the foundation for specific targeted therapy.

1.3 The PI3K – Akt - mTOR pathway

The mTOR (mammalian target of rapamycin) cell signaling pathway is an important central pathway that integrates the signals from nutrients and growth factors to regulate cell proliferation and homeostasis in most multicellular organisms. Over the last decade, clinical interest has been intensified in the mTOR pathway as it has been shown to be dysregulated in diseases such as type 2 diabetes and cancer. [Laplante, M. 2009]. The mTOR protein is an evolutionarily conserved, 289-kD serine/ threonine protein kinase that belongs to the phosphoinositide 3-kinase (PI3K)-related kinase family. mTOR is a central component of two distinct multi-protein complexes named mTOR complex 1 (mTORC1) and 2 (mTORC2) (Fumarola et al. 2014).

mTORC1 consists of at least six proteins: the catalytic subunit, mTOR; the regulatory-associated protein of mTOR (Raptor), mLST8 or mammalian lethal with Sec13 protein 8 (also known as GβL), PRAS40 or proline rich Akt substrate 40 kDa, Deptor or DEP-domain-containing mTOR-interacting protein, and the Tti1/Tel2 complex (Laplante and Sabatini 2012). The exact functions of most of the mTORC1 complex components are still unclear. Several studies have suggested that the regulatory protein Raptor might play a role in the recruitment of substrates for mTOR and regulating assembly and mTORC1 activity (Kim et al. 2002, Hara et al. 2002). PRAS40 and Deptor serve as negative regulators of mTORC1. When the activity of mTORC1 is reduced, PRAS40 and Deptor are recruited to the complex (Wang et al. 2007), where they promote the inhibition of mTORC1. Akt directly phosphorylates PRAS40 and Deptor to reduce their physical interaction with the kinase which leads to further activation of mTORC1 signaling (Peterson et al. 2009, Wang et al. 2007). The role of mLST8 protein is not yet characterized and in vivo

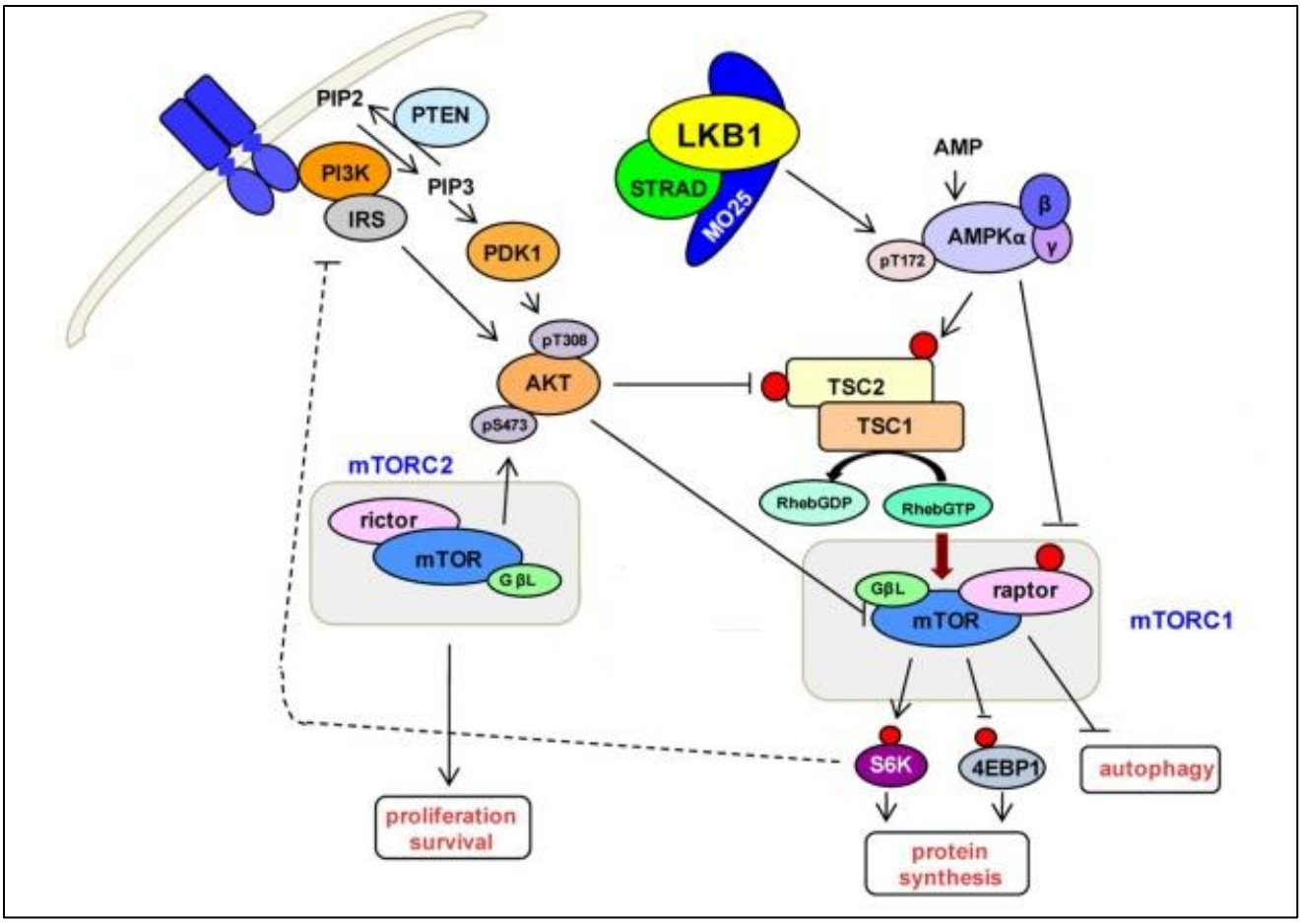

Figure 2: The mTOR signaling pathway (Andrade-Vieira et al. 2013). LKB1 is also known as STK11 (see figure 1). It should be noted that mTOR signaling is tightly regulated by a feedback loop via S6K1 phosphorylation of IRS.

deletion of mLST8 does not alter mTORC1 activity (Guertin et al. 2006). Recent findings suggest that the novel mTOR binding protein Tti1 along with its binding partner Tel2 play an important role in the mTOR activity through maintenance of the complex assembly (Kaizuka et al. 2010). mTORC1 integrates signals from the extracellular environment such as growth factors, nutrients and energy sources to regulate cell survival, growth and proliferation by stimulating anabolic processes such as lipid and protein biosynthesis, and limiting catabolic processes like autophagy (Shimobayashi and Hall 2014).

The mTOR signaling pathway is much more complex than originally thought and much of its understanding has come from the use of a bacterial macrolide Rapamycin. Rapamycin forms a complex with the FK506-binding protein of 12 kD (FKBP12) which interacts with the FKBP12- rapamycin binding domain (FRB) of mTOR, and leads to inhibition of mTORC1. It is still unclear how the inhibition of mTORC1 by FKBP12 takes place but it is speculated that rapamycin allosterically inhibits the kinase activity; but it has also been suggested that this is caused by an alteration in the structural integrity of mTORC1(Laplante and Sabatini 2012).

Among the multiple functions of mTORC1, the best-characterized function is regulation of translation. It does so via two downstream mediators, the eukaryotic initiation factor 4E (eIF4E)-binding protein 1 (4E-BP1) and the p70 ribosomal S6 kinase 1 (p70S6K1, S6K1). mTORC1 directly phosphorylates 4E-BP1 and prevents its binding to the cap-binding protein eIF4E, thus allowing eIF4E to initiate cap-dependent translation. The activation of the serine-threonine kinase, S6K1, by direct phosphorylation by mTORC1 leads to biogenesis of mRNA as well as initiation of translation and elongation and is mediated via direct phosphorylation of 40S ribosomal protein S6 by S6K1 (Ma and Blenis 2009). Thus phosphorylation of S6K1 by mTORC1 directly stimulates the assembly of the complex needed for cap-dependent translational initiation while phosphorylation of 4EBP1 removes an inhibitor of this process.

The majority of extracellular signals that regulate mTORC1 are transmitted through the key upstream heterodimer complex, the tuberous sclerosis 1 (TSC1; or hamartin) and TSC2 (also known as tuberin)

proteins, which has a GTPase-activating protein (GAP) domain functioning as a negative regulator of the Ras homolog enriched in brain (Rheb). Rheb, in its GTP-bound form, is active at stimulating mTORC1 activity. Exactly how this activation takes place is yet to be determined but it is thought to be mediated via phospholipase D1 interaction with Rheb-GTP (Groenewoud and Zwartkruis 2013). The TSC1/2 complex negatively regulates mTORC1 activity by stimulating the conversion of Rheb-GTP to Rheb-GDP resulting in subsequent inhibition of mTORC1. In conditions of energy stress, the TSC1/2 complex is activated by the AMP-dependent kinase (AMPK) resulting in mTORC1 inhibition (see section 1.5), whereas mitogenic signals inhibit AMPK-mediated TSC1/2 phosphorylation and promote mTORC1 activity leading to cell growth and proliferation. The TSC1/2 complex serves as an integration node where many of the upstream signals converge to regulate mTORC1 activity. The activation of membrane receptors, including receptor tyrosine kinases (RTKs) EGFR, VEGFR, HER2, IGFR-1, and PDGFR recruits the kinase PI3K to the cell membrane. PI3K phosphorylates phosphatidylinositol lipid substrates in the plasma membrane to generate PIP3 from PIP2. PIP3 further recruits and activates a number of proteins containing the pleckstrin homology (PH) domain including phosphoinositide-3-kinase-family member kinase B/Akt (PKB/Akt) and phosphoinositide-dependent protein kinase-1 (PDK1). PDK1 can further phosphorylate Akt and other substrates including serum/glucocorticoid-regulated kinase 1 (SGK1), and ribosomal S6 kinase 90 kD, polypeptide 1 (RSK1). Phosphorylation of Akt at T308 by PDK1 alone does not activate it, but it needs an additional activating phosphorylation from mTORC2 at residue Ser473 for full activation (Martinez et al. 2008). Akt in its active form can activate mTORC1 by direct inactivating phosphorylations of PRAS40 and TSC2 (Fumarola et al. 2014, Martini et al. 2014).

The mTOR complex 2 consists of at least seven known components: mTOR, rapamycin-insensitive companion of mTOR (Rictor), mammalian stress-activated MAP-kinase interacting protein (mSIN1), and protein observed with Rictor 1 and 2 (Protor-1/2), mLST8, Deptor and the Tti/Tel2 complex. Evidence suggests that Rictor and mSIN1 stabilize each other to form the structural foundation of mTORC2. Rictor also interacts with Protor-1, but the physiological functions of this interaction are not yet established.

Similar to its role in mTORC1, Deptor negatively regulates mTORC2 activity and is the only characterized endogenous inhibitor of mTORC2 so far discovered. In contrast to its role in mTORC1, mLST8 is essential for mTORC2 function; knockout of this protein severely alters the stability and the activity of this complex. Much less is known about mTORC2 compared to mTORC1. However, recent studies have demonstrated that mTORC2 is a key mediator in several biological processes such as cell growth and proliferation, the function of the cytoskeleton machinery, and metabolism (Laplante and Sabatini 2009).

Although mTORC2 is insensitive to rapamycin, prolonged exposure to rapamycin or its analogs suppresses mTORC2 activity by disturbing the assembly of this complex. mTORC2 does not directly respond to signals from nutrients, but studies have shown that mTORC2 can be activated by growth receptors like the insulin receptors by a PI3K mediated pathway whose mechanism is not clear. The absolute necessity of ribosomes for the activation of mTORC2 (Zinzalla et al. 2011) suggests that the PI3K related pathway could be ribosome-dependent. mTORC2 phosphorylates Akt at Ser473 which results in complete activation of Akt; lack of Akt phosphorylation by mTORC2 impedes phosphorylation of some Akt substrates like Forkhead Box O1/3a (FoxO1/3a) but not TSC2 and GSK3. mTORC2 also directly activates serum- and glucocorticoid-induced protein kinase 1 (SGK1) that regulates ion transport and growth. It also phosphorylates a third protein kinase Cα (PKCα) and other effectors like paxillin and Rho- and Rac–GTPases to control the actin cytoskeleton.(Laplante and Sabatini 2012). Despite the advances in the mTOR field, the understanding of mTORC2 is limited and additional work is needed to evaluate the biological functions of mTORC2 and its interaction with mTORC1.

1.4 Feedback circuit controlling signaling to mTORC1

The mTOR pathway is subject to very tight regulation via several positive and negative loops. One of the best characterized loops is a S6K1 mediated negative feedback on PI3K. S6K1 phosphorylates a growth factor receptor adaptor protein IRS-1, to inhibit it and induce its degradation, which dampens the PI3K –

Akt pathway (see Figure 2). The importance of this feedback became clear from the reactivation of signaling to mTORC1 following rapamycin-induced inhibition of S6K1 phosphorylation (O'Reilly et al. 2006). mTORC1, specifically, is regulated by a positive feedback through mTORC2 which phosphorylates Akt to reinforce Akt/mTORC1 signaling. These positive and negative feedback loops have a crucial importance clinically as responses to mTOR inhibitors are currently thought to be limited by their operation.

1.5 LKB1- AMPK - mTOR Signaling Pathway

AMPK is a sensor molecule of cellular energy status that maintains cellular energy homeostasis, and is thought to have evolved in the cellular response to energy stress (Hardie 2011). It also has distinct roles in mitochondrial biogenesis and disposal, autophagy, and cell growth and proliferation. It senses an increase in cellular AMP: ATP ratio and is activated by metabolic stresses that inhibit ATP production or accelerate ATP consumption (Hardie 2011). Upon activation, AMPK regulates several downstream processes that inhibit cell growth and proliferation. AMPK comprises of three subunits: the catalytic α subunit, the structural scaffold β subunit, and the regulatory γ subunit. The α subunit contains the kinase domain with a conserved threonine residue at codon 172 that is phosphorylated by the upstream kinases in the activation loop (Hardie 2011). The binding of AMP (or AMP-mimetic ZMP) causes a conformational change in the γ subunit of AMPK that leads to the phosphorylation of the α subunit at T172. This phosphorylation is crucial for the activity of AMPK. The main upstream kinase that phosphorylates AMPK at T172 is a serine/threonine kinase LKB1 (Liver kinase B1or STK11). The discovery of LKB1 first introduced the connection between AMPK and cancer. LKB1 was originally discovered as a tumor suppressor gene responsible for an inherited susceptibility to cancer, the Peutz-Jeghers syndrome, and now is found to be mutated in almost 30% of NSCLC (Han et al. 2013). LKB1 is active as a heterotrimeric complex (see Figure 2). It is unclear if the tumor suppressor functions of LKB1 are mediated via AMPK because, in addition to AMPK, LKB1 activates another 12 AMPK-related kinases

whose functions are poorly defined (Shackelford and Shaw 2009). The effects of AMPK in regulating cell growth and proliferation have been extensively studied. Once activated, AMPK causes p53 dependent cell cycle arrest by inhibiting major biosynthetic pathways responsible for synthesis of fatty acids, phospholipids, proteins, and ribosomal RNA. AMPK T172 can also be phosphorylated by CAMKKβ in the presence of Ca^{+2} or a calcium ionophore, but absence of AMP. In conditions of stress, AMPK regulates cellular processes by acting on mTORC1 signaling with a dual mechanism that inhibits mTORC1 activity via direct phosphorylation of TSC2 and of Raptor (Inoki et al. 2003). AMPK phosphorylation of TSC2 activates the conversion of Rheb-GTP to Rheb-GDP leading to subsequent inhibition of mTORC1. Phosphorylation of Raptor at two conserved serine residues causes to downregulation of mTORC1 activity (Gwinn et al. 2008).

AMPK is also a direct regulator of autophagy (Hoyer-Hansen and Jaattela 2007). Autophagy is a cellular process of engulfment of cytoplasmic components that are dysfunctional or in surplus by vacuoles which fuse with lysosomes to form autophagosomes. This process is of importance during cellular starvation as a means to recycle amino acids for the conservation of vital proteins (Hardie 2011). It also has implications in cancer biology and serves to prevent accumulation of damaged organelles and proteins. AMPK, under glucose starvation, phosphorylates UNC-51-like kinases 1/2 (ULK1/ULK2) – the protein kinases located at the top of the autophagy cascade promoting autophagosome formation and autophagy. In the absence of AMPK mediated mTORC1 inhibition, mTORC1 1 phosphorylates ULK1 at multiple sites to prevent its interaction with AMPK and thus inhibits autophagy (Fumarola et al. 2014).

1.6 Current chemotherapy for NSCLC

Treatment for NSCLC is based mainly on the stage of the cancer and how far it has spread. Generally, early stage cancer does not invade other tissues and is localized at the primary site. It is most often treated by surgery alone, and does not require radiation or chemotherapy. In some cases though, radiation or chemotherapeutic intervention is required in order to kill residual tumor cells left by surgery. Stage 1 and

stage 2 NSCLCs are still localized, and are treated by surgery, radiation, chemotherapy or a combination of these methods. Stage 3 – 4 NSCLC is considered to have spread extensively to several lymph nodes or to have metastasized and invaded other tissues. Treatment options in such cases depends on patients overall health, size of tumor, the extent of spread and how well an individual can tolerate a particular treatment. Stage 4 tumors are widely spread when diagnosed, and are very hard to cure. Therapeutic interventions may prolong the life of the individuals and relieve symptoms, but aren't likely to result in cures of advanced stage NSCLC (Ettinger et al. 2012).

The first line of chemotherapeutic treatment for NSCLC is platinum based therapy with overall response rate of 25%-35% and median survival of 8-10 months (Kawabata et al. 2014). Unfortunately, this effect plateaus off. Several studies have combined cisplatin, carboplatin and oxaliplatin with targeted compounds like bevacizumab (Peters et al. 2012). However, the usage of these combinations is limited to certain genotype and also has severe toxicity profiles. The best chemotherapy regimen for advanced NSCLC still remains unclear. The US Food and Drug Administration approved pemetrexed for the treatment of pleural mesothelioma in 2004. Pemetrexed in combination with cisplatin was approved for first-line treatment of NSCLC in 2008 (Scagliotti et al. 2008), and, notably, for maintenance therapy of NSCLC in 2009, the first drug ever approved for this purpose (Owonikoko et al. 2010). PTX inhibits thymidylate synthase (Taylor et al. 1992, Shieh et al. 1998) but also has a second mechanism: activation of the AMP-dependent protein kinase (AMPK) via inhibition of AICART (Racanelli et al. 2009). Monotherapy has not been much effective in treating NSCLC and, when pemetrexed alone was compared to carboplatin and pemetrexed in population of 217 patients, the combination therapy demonstrated higher therapeutic efficacy over the single agent (Peters et al. 2012).

Recent approaches to treat NSCLC use targeted agents. In NSCLC with EGFR mutations, tyrosine kinase inhibitors (TKIs) are prescribed as first-line agents (Zhou et al. 2011). Studies have shown that erlotinib (Tarceva) helps to control certain lung tumors, especially in women and in people who have never

smoked. Cetuximab is another drug that targets EGFR. In patients harboring mutations in the ALK gene, crizotinib (Xalkori) can shrink tumors and has been shown to provide good outcomes (cancer.org).

1.7 Activators of AMPK

A fundamental trait of all multicellular eukaryotic cells is that they integrate the signals from nutrients and growth factors to drive cell proliferation and growth, only when the supply of nutrients is sufficient and cell division can be successfully completed. The signals from the energy stores and nutrients are transmitted via a sensor molecule AMPK, which is activated when intracellular levels of ATP decline and that of AMP rise. Activation of AMPK by increase in the levels of AMP is a signal that cellular energy stores are depleted and cell proliferation has to stop. LKB1 phosphorylates the AMPK activation loop on AMPKα in conditions of energy stress and controls cell growth and proliferation via effects directly on mTORC1; mTORC1 being one of the major mediators of cell growth and proliferation. Thus, one would expect that activation of AMPK can be explored as one of the potential mechanisms to inhibit cell proliferation and survival, a desirable strategy for the treatment of cancer.

Given its role in metabolic physiology, AMPK has garnered interest as a target for the treatment of type 2 diabetes and other metabolic diseases such as obesity, cardiovascular disease and fatty liver disease. AMPK regulates glucose homeostasis by balancing glucose uptake and production (Kurth-Kraczek et al. 1999). It promotes glucose uptake by stimulating glucose transporter 4 (GLUT4) to translocate from intracellular storage vesicle to the plasma membrane, an effect thought to be mediated via Rab GTPase-activating protein AS160 and TBC1D1. The AMPK activator, 5-amino-4-imidazolecarboxamide ribonucleoside (AICAR), has been shown to increase glucose uptake and translocation of GLUT4 to plasma membranes in skeletal muscle of rat (Lin et al. 2014). Metformin and thiazolidinedione's, which are type 2 anti-diabetic drugs, inhibit hepatic gluconeogenesis by activation of AMPK, thereby downregulating expression of gluconeogenic genes such as phosphoenolpyruvate carboxykinase (PEPCK) and glucose-6-phosphatase (G6Pase) (Lin et al. 2014).

At least 33 AMPK activators have been identified so far (Lin, Chen et al. 2014). Metformin, phenformin, and AICAR have been shown to activate AMPK and suppress growth of tumor cells in culture and in rodent cancer model xenografts. It has been shown that diabetics treated with metformin, which indirectly activates AMPK, had a lower incidence of cancer than patients on other anti-diabetic therapies and studies are being done to examine the effect of Metformin on cancer incidence (Han et al. 2013). AICAR is directly converted to aminoimidazolecarboxamide ribonucleotide (ZMP) – an AMP mimetic, via adenosine kinase, and the accumulating ZMP activates AMPK to control cell growth and inhibit proliferation through mTORC1inhibition (Racanelli et al. 2009). In this laboratory, Rothbart et al (2010) have shown that pemetrexed, an anti-folate, indirectly activates AMPK in human carcinomas. They showed that pemetrexed inhibits the second folate-dependent enzyme of de novo purine synthesis, aminoimidazolecarboxamide ribonucleotide formyltransferase (AICART) in human leukemic cells. Inhibition of AICART leads to accumulation of its substrate ZMP which in turn activates AMPK (Racanelli et al. 2009, Rothbart et al. 2010).

Current evidence suggests that AMPK activation inhibits major biosynthetic pathways in the cells and controls cell survival, growth, and proliferation. These effects enforce a metabolic checkpoint on the cell cycle suggesting that AMPK activators deserve further investigation as cancer therapeutics (Jones et al. 2005). However, a study by Huang et al. (2008) showed that although AMPK activators delayed tumorigenesis, all of the mice eventually developed tumors. One plausible explanation to explain how tumor cells escape the cytostatic effects of AMPK activators could be that they acquire additional mutations, e.g.: loss of the LKB1 gene that prevents continued AMPK activation (Sanchez-Cespedes et al. 2002). This suggests that AMPK activators are likely to be most effective when used in combination with other targeted therapeutics.

An important fact to note here is the existence of an energy associated growth suppressor pathway mediated by AMPK capable of suppressing cancer growth and, possibly, its development. This point outs that diet and exercise might be correlated with cancer incidence rates; and it has been suggested that

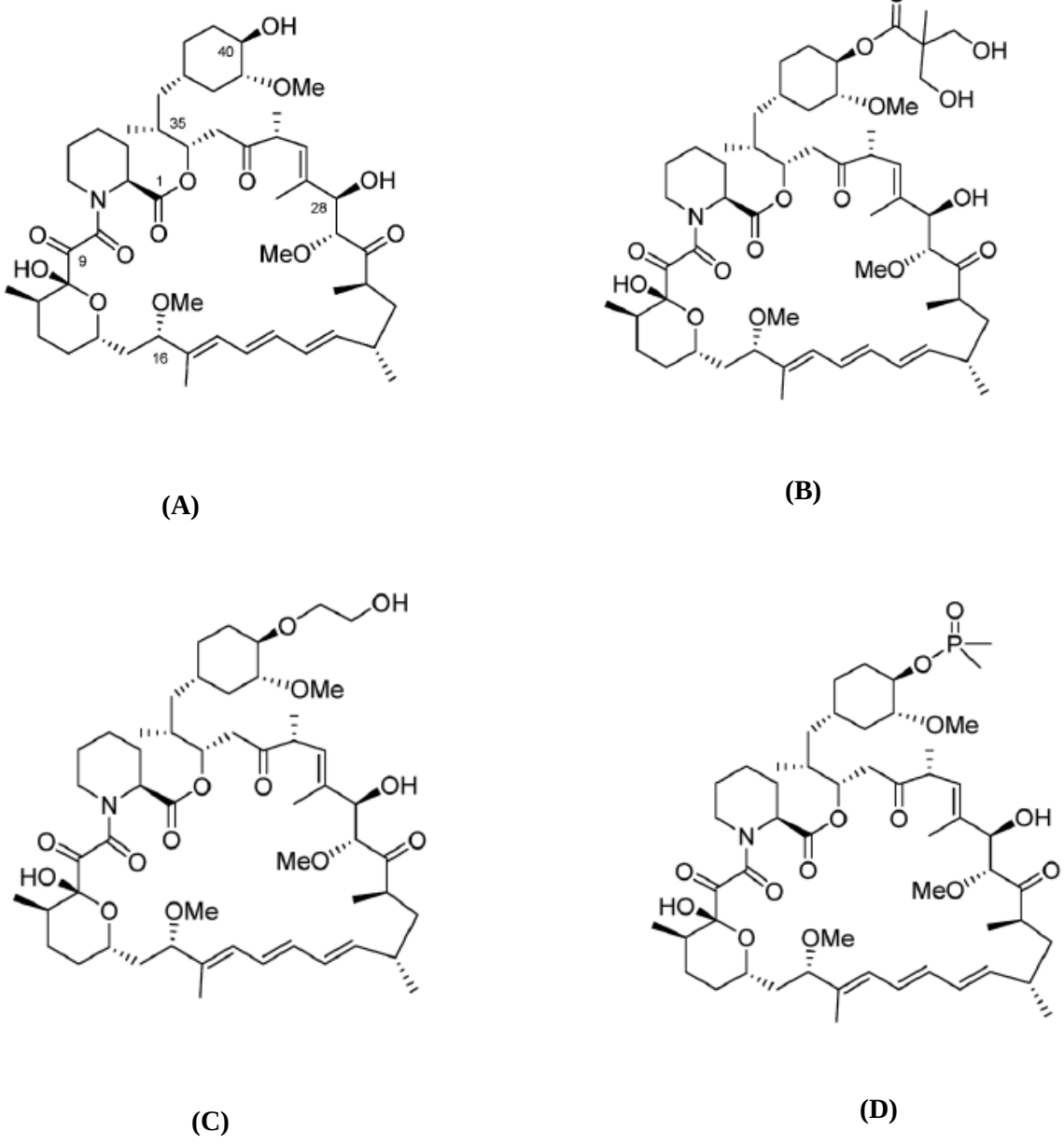

Figure 3: Structures of rapamycin and its analogs: Rapamycin (A), temsirolimus (B), everolimus (RAD001; C), and ridaforolimus (D).

dietary factors might contribute to an estimated one-third of all cancer deaths (Martinez et al. 2008). It has been seen from a number of epidemiologic studies that cancer risk is higher amongst people with metabolic syndrome, or obesity, or type 2 diabetes. A recent study has shown that AMPK was activated and mTORC1 signaling was suppressed in rodent tissues in a dose-dependent manner by increasing the levels of dietary restriction (Shaw 2009).

Taken together, activation of AMPK- either directly or indirectly by PTX-mediated AICART inhibition regulates mTORC1 function along with other important cellular processes. These processes are most frequently deregulated in cancer, prompting studies to evaluate the anti-tumor effects of activators of AMPK.

1.8 mTOR inhibitors

1.8.1 First generation mTOR inhibitors: Rapamycin and its analogs

The first mTOR inhibitor to be discovered was rapamycin, a macrolide antibiotic produced by *Streptomyces hygroscopicus*. Rapamycin strongly inhibits T-cell proliferation and was approved by FDA in 1999 as an immunosuppressant to prevent organ transplant rejection (Sehgal 2003). Rapamycin allosterically inhibits mTORC1 through the FRB domain (see section 1.3) while mTORC2 is insensitive to rapamycin. It has been shown that rapamycin acts by blocking G1 cell cycle progression (Sehgal 2003). Several studies have also shown that rapamycin induces apoptosis through inhibition of hypoxia-induced increases in hypoxia-inducible factor 1α (HIF-1α) (Houghton 2010). It also induces autophagy and enhances radiation therapy when combined with a Bcl-2 inhibitor that concurrently induces apoptosis (Fumarola et al. 2014). However, the effects of rapamycin are generally confined to a cytostatic effect and the clinical use of rapamycin as an anti-tumor agent is limited (Guertin and Sabatini 2009). This therapeutic limitation is thought to be because of its inability to inhibit mTORC2, and the activation of Akt kinase following initial inhibition of mTORC1. Inhibition of mTORC1 results in feedback induction of IRS-1 expression and activation of IGF-I signaling; thus reducing the antitumor effects of mTORC1

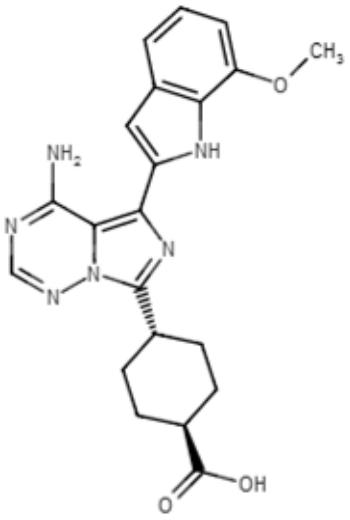

(A)

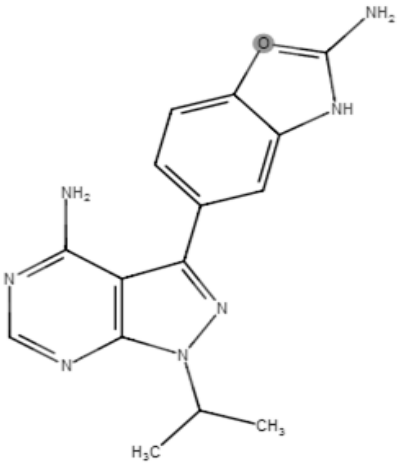

(B)

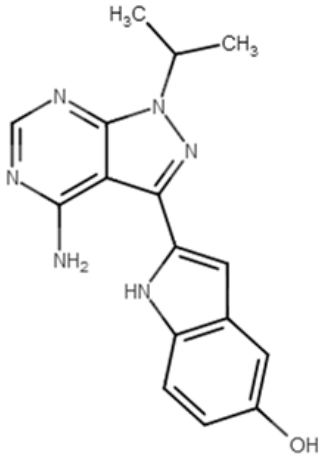

(C)

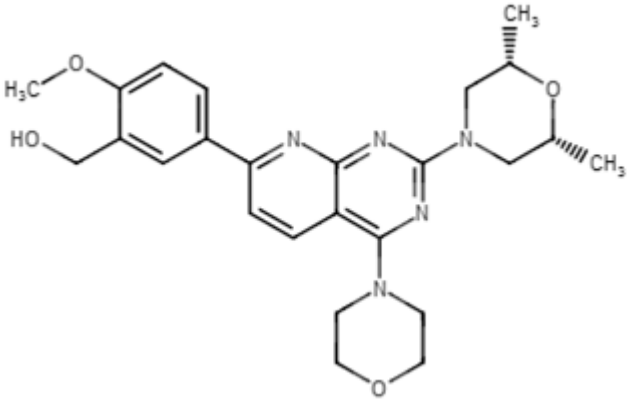

(D)

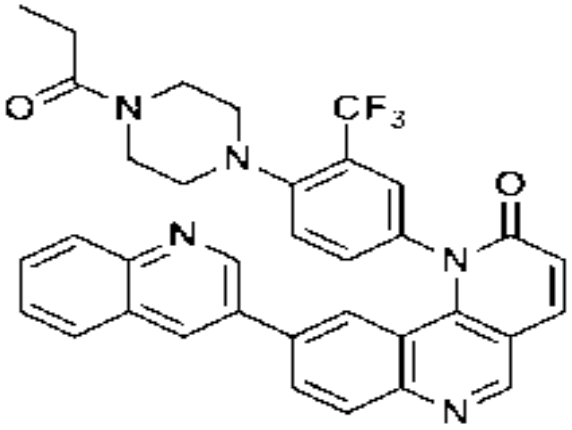

(E)

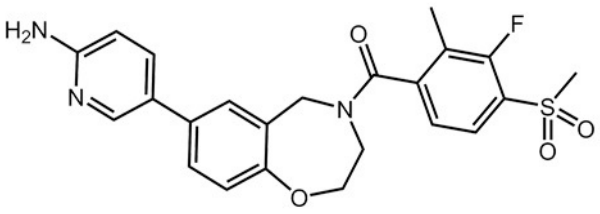

(F)

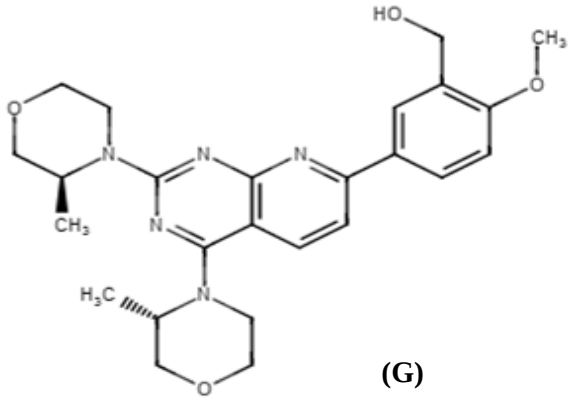

(G)

Figure 4: Structures of second generation mTOR inhibitors: OSI-027 (A), INK-128 (B), PP-242 (C), KU0063794 (D), Torin (E), XL-388 (F), and AZD8055 (G).

inhibitors (O'Reilly et al. 2006) (see Figure 2). Rapamycin treatment induces IRS-1 expression due to inhibition of p70-S6K1 phosphorylation, which results in increased IGF-IR/IRS-1/PI3K signaling to Akt. Reports have shown that p70- S6K mediates phosphorylation of IRS-1 inhibitory serine sites (Ser312 and/or Ser636/639) which lead to IRS-1 degradation (Manning 2004). Thus, suppression of p70-S6K1 activity by rapamycin may prevent inhibitory IRS-1 phosphorylation, thereby stabilizing IRS-1. An increase in IRS-1 adapter protein levels is thought to induce Akt activity by augmenting IGF-IR signaling to PI3K/Akt (Shi et al. 2005). Hence, combining rapamycin with inhibitors of IGF-IR or Akt seems to be a good therapeutic strategy and this approach is under investigation (Wan et al. 2007). Currently, rapamycin is only active against certain tumors such as mantle cell lymphoma, renal cell carcinoma and endometrial cancer, in which it is thought to block the effects of mTORC2 by some unexplained mechanism (Liu et al. 2009).

Owing to poor water solubility, Rapamycin has a low bioavailability. Hence, several analogs of rapamycin with better pharmacokinetic profiles, collectively called "rapalogs", have been developed. They include Everolimus (RAD001/Affinitor), Temsirolimus (Toricel) and Ridaforolimus (MK-8669) (Figure 3); all of these analogs appear to have the same mechanism of action as rapamycin. Everolimus, originally commercialized as an immunosuppressant, was recently approved for the treatment of advanced renal carcinoma by the US FDA. A recent study has demonstrated that, in addition to mTORC1 inhibition, everolimus inhibits the response of vascular endothelial cells to stimulation by vascular endothelial growth factor (VEGF) and that its anti-tumor effects are attributed to its anti-angiogenic properties (Houghton 2010). Temsirolimus is a prodrug of rapamycin and is converted to rapamycin in vivo. Ridaforolimus is still under phase III clinical trials for a variety of cancers that include advanced malignancies such as metastatic soft tissue and bone sarcoma, breast cancer, and relapsed hematological malignancies (Liu et al. 2009).

Rapalogs, like rapamycin, have shown significant activity in clinical trials but their activity is also limited to inhibition of mTORC1. The rapalogs exhibit a cytostatic effect on tumor growth suppression and

cancer disease stabilization, rather than regression (Meric-Bernstam and Gonzalez-Angulo 2009). To circumvent this, they have been combined with other chemotherapeutic agents and better therapeutic efficacies have been observed with combinations over single drug treatment. For instance, the combination of antiestrogen ERA-923 with temsirolimus has been reported for treating breast cancer (Sadler et al. 2006). Rapalogs are also been combined with Insulin-like growth factor I receptor (IGF-IR) inhibitors because of the rapalog-induced Akt activation (feedback loop) observed in cancer cell lines in vitro and in clinical trials (Shi et al. 2005, O'Reilly et al. 2006). Other studies have reported the evaluation of combination of rapalogs with PI3K inhibitors NVP-BKM120 and XL-765 (SAR245409), the Akt inhibitors like GSK690693 and Perifosine, inhibitors of the RAS/RAF/MEK pathway, and other targeted agents. Each of these combinations has been shown to enhance therapeutic efficacy in preclinical models (Liu et al. 2009).

1.8.2 Second generation mTOR inhibitors: Catalytic site (ATP-competitive) inhibitors

Despite the preclinical promise shown by rapalogs, the clinical utility for rapalogs has been limited to a few cancers. Tumor relapse is often observed with rapalogs due to their selectivity for mTORC1 inhibition and the effect of the negative feedback loop on IRS-1. Although they cause a marked hypophosphorylation of S6K1, rapalogs fail to sustain the dephosphorylation and inhibition of 4EBP1, and cell proliferation persists even in the presence of the drug (Fumarola et al. 2014). Interestingly, rapalogs exhibit strong inhibitory activity towards one mTORC1 substrate S6K1, while inhibition of 4E-BP1 is minimal, indicating that it could be an important mechanism of drug resistance. In order to overcome these limitations, novel dual mTORC1/2 inhibitors have been developed and are being studied extensively. These compounds (Figure 4) bind to the catalytic domain of mTOR, and inhibit the mTOR kinase activity, thus effectively inhibiting both mTORC1 and mTORC2 (Chresta et al. 2010). The inhibition of mTORC2 is thought to prevent feedback induction of Akt (Hsieh et al. 2012). These ATP-competitive inhibitors are highly potent at inhibiting mTORC1 and mTORC2 such that they exhibit inhibitory concentrations (IC_{50}) in vitro in the low nanomolar range as determined by S6K1

phosphorylation at T389 and Akt phosphorylation at S473, respectively. They are also very selective such that structurally related kinases are inhibited only at much higher concentrations of drug (Guertin, and Sabatini 2009).

Torin 1 was one of the first dual mTORC1/2 inhibitor developed. It is shown to inhibit proliferation of primary tumor cells to a greater extent than rapamycin (Liu et al. 2009). Shokat and his colleagues have developed PP242 and PP30, both ATP-site mTOR inhibitors exhibiting similar therapeutic profiles to that of Torin1 (Liu et al. 2009). It was assumed that these drugs presented greater therapeutic efficacies than rapalogs because of their ability to inhibit both mTORC1 and mTORC2. Interestingly, it was observed that, in addition to mTORC2 inhibition, the anti-tumor effects of PP242 and PP30 are mediated via more-complete inhibition of mTORC1 leading to sustained dephosphorylation and inhibition of 4EBP1 and cap-dependent mRNA translation (Feldman et al. 2009). A number of mTOR catalytic site inhibitors are under preclinical and phase I/II trials and have shown remarkable potency and selectivity for mTORC1 and mTORC2 (Liu et al. 2009). These include KU0063794 (AstraZeneca), INK-128, XL388, OSI-027 and AZD8055. These compounds are under investigation for NSCLC and have demonstrated superior efficacies compared to rapamycin and its analogs in preclinical testing (Liu et al. 2009, Guertin and Sabatini 2009, Fumarola et al. 2014, Hsieh et al. 2012).

AZD8055 is a particularly interesting member of this family of drugs. It is an orally bioavailable, potent, and selective mTOR kinase inhibitor with excellent selectivity for these kinases and modest activity against all class I PI3K isoforms and other members of the PI3K-like kinase family. AZD8055 has shown proven efficacy in NSCLC cell lines superior to that of rapamycin (Guertin and Sabatini 2009). AZD8055 has been shown to significantly decrease the phosphorylation of 4EBP1 on the rapamycin-insensitive T37/46 sites and to potently inhibit cap-dependent translation at low nanomolar concentrations with concomitant inhibition of cell proliferation. It is also thought to promote a greater autophagosome formation and autophagy activation than rapamycin. In addition, AZD8055 induced significant growth inhibition and regression in NSCLC xenografts (Fumarola et al. 2014). Similar to the rapalogs, catalytic

site mTOR inhibitors have also been combined with inhibitors of the PI3K-Akt pathway to overcome the negative feedback of mTORC1 inhibition on PI3K/Akt and MAPK signaling (Liu et al. 2009, Guertin and Sabatini 2009). AZD8055, in combination with MEK 1/2 inhibitor AZD6244 (selumetinib) has demonstrated superior anti-tumor efficacy over either drug given as single agents (Fumarola et al. 2014).

Some ATP- competitive inhibitors show dual activity against mTORC1/2 as well as activity against the p110 subunit of PI3K due to the structural similarity of the catalytic domains of these proteins, and are called dual mTOR-PI3K inhibitors. These agents have the potential of completely shutting down the PI3K/Akt/mTOR pathway but it may cause greater toxicity. Examples of this class of drugs are NVP-BEZ235 and XL-765 (SAR245409); these compounds are currently under phase I/II clinical trials for NSCLC and breast cancer (Liu et al. 2009, Fumarola et al. 2014).

1.9 Combination therapy for cancer

Combination therapy refers to the use of more than one drug at a time for treating a disease. As often observed with other chemotherapies, most cancers become resistant to one drug and the clinical response declines or stops. Most often an initial responsive tumor becomes refractory and starts growing again over a period of time. This is thought to be attributed to inherent resistance of the tumor cells due to pre-existing mutations. Under typical conditions, a tumor mass of 10^9 cells has 1000-10000 inherently resistant cells which have the potential to repopulate and bring about a recurrence of tumor. Under such conditions, there is a great need for multidrug therapy. The rationale for combination therapy is to use drugs that act on different targets and by different mechanisms to manage the heterogeneity of cancer cells, thereby decreasing the likelihood of developing resistant cancer cells. Another benefit of using combination therapy is that each drug can be given at lower concentrations than as single agents, thus reducing events of toxicity.

A tumor is a population of cells that have undergone genetic alterations and have gained capacity to grow and proliferate uncontrollably. These genetic mutations are most often observed in the signaling pathways

that control cellular survival in response to nutrients and energy. Aberrations in one or more proteins that control growth and homeostasis, belonging to different signaling pathways leads to continuous signaling inputs, thereby causing tumors to arise. Heterogeneity among tumor cells increases the number and diversity of potential target sites for chemotherapy and the need for combining therapeutic agents. The main aim of a combination therapy is to achieve increased therapeutic efficacy with a combination of drugs over that achievable with the individual agents, providing selective synergism against the tumor, and to minimize outgrowth of drug-resistant tumor clones.

1.10 Hypothesis

The PI3K-Akt-mTOR cell signaling pathway transmits signals from nutrients and controls cell survival and growth. On the other hand, the LKB1-AMPK-mTOR axis of the mTOR pathway recognizes cellular energy levels and responds to energy stress to regulate cell growth and proliferation. Thus, the PI3K-Akt-mTOR and LKB1-AMPK-mTOR axes, that are crucial for cell survival and growth mechanisms, converge on the mTOR protein which has been validated as a promising target for cancer therapy. An activator of AMPK, pemetrexed, is approved as a first line drug in combination with cisplatin for the treatment of NSCLC. Pemetrexed exerts its effects via a) inhibition of TS, and b) AMPK mediated mTORC1 inhibition. Studies have showed that the combination of pemetrexed with targeted agents such as bevacizumab have shown better therapeutic profiles over the single agents. Rapamycin and its analogs inhibit mTORC1 activity and have emerged as first generation mTOR inhibitors. RAD001 is FDA approved in renal cell cancer. However, due to their inhibitory effect on mTORC1, they have shown a more modest clinical response than expected. A newer generation of mTOR antagonists known as "catalytic site" mTOR inhibitors, target both mTORC1/2 and are expected to have superior efficacy than the rapalogs. They are currently under phase I/II clinical trials. We proposed to experimentally determine whether an AICART inhibitor (AMPK activator) would enhance the activity of direct mTOR inhibitors and vice-versa. We hypothesized that the dual mTOR antagonists, which inhibit the ATP-site of

mTORC1/2, would have an additive or synergistic interaction with an activator of AMPK, which endogenously inhibits mTORC1 signaling through TSC1/2 and raptor phosphorylation. Dual mTOR inhibitors would control the feedback loops that regulate mTOR activity and thereby suppress the PI3K-Akt-mTOR signaling, whereas an AMPK activator (Pemetrexed) would regulate endogenous growth signals through mTORC1 inhibition. Combining the two effects is a promising strategy in order to achieve anti-cancer activity.

Chapter 2: Materials and Methods

2.1 Cell lines, chemicals and reagents

NSCLC cell lines H661, H441 and H358 were purchased from American Type Culture Collection (Manassas, VA) and kept under liquid nitrogen in 10% DMSO (Sigma Chemicals, St. Louis, MO) and 90% Fetal Bovine Serum (FBS; Atlanta Biologicals) until use. Pemetrexed disodium (LY231514) was obtained from Eli Lilly and Company (Indianapolis, IN) and a stock solution of 1 mM was prepared by dissolving 5.16 mg PTX in 10 ml 1X phosphate buffered saline (PBS, Cat #10010, pH 7.4; Gibco, Life Technologies, NY, USA). AICAR (Cat #A611700) was obtained from Toronto Research Biochemicals (North York, Ontario, Canada) and a stock solution of 40 mM was prepared by dissolving 103.2 mg of AICAR in 10 ml 1X PBS. RAD001(Cat # S1120; Everolimus; Novartis) and AZD8055 (Cat # S1555; AstraZeneca), were purchased from Selleck Chemicals and were dissolved in dimethyl sulfoxide (DMSO) as stock solutions at 20mM and 10 mM, respectively. All drug stock solutions were stored at -20^{0}C until use. Stock solutions of thymidine (560 μM) were routinely made by dissolving 0.00678 g of thymidine powder in 48 ml of 1X PBS. The concentration was determined by measuring absorbance at 267 nm from a 1:10 dilution of the stock solution in 1X PBS using an extinction coefficient of 9.7 mM^{-1} cm^{-1}. The volume was adjusted accordingly with 1X PBS for a final concentration of 560 μM. This solution was filter-sterilized and was stored at -20°C. Unless otherwise noted, thymidine was typically used at a final concentration of 5.6 μmol/L in rescue experiments. Complete EDTA-free Protease Inhibitor Cocktail tablets (Cat #11873580001) were from Roche Applied Science (Indianapolis, IN). Bio-Rad dye concentrate (Cat # 500-0006), 30% Acrylamide/BIS solution 37.5:1 (Cat #1610158), Laemmli Sample Buffer (Cat #1610737), and Dual Color Precision plus Protein Standard (Cat #1610374) were from Bio-Rad Laboratories. Immobilon polyvinylidene fluoride (PVDF) membrane (Cat #IPVH00010) was from Millipore (Billerica, MA). StartingBlock Blocking Buffer (Cat #37542), goat anti-rabbit IgG (Cat #31462), and goat anti-mouse IgG (Cat #31348) secondary antibodies were from Thermo Scientific. A list

of antibodies and their sources can be found in Table 1. All other reagents were from Fisher Scientific (Waltham, MA) or Sigma Aldrich (St. Louis, MO) and were of the highest available purity.

2.2 Cell Culture

Cells were grown from frozen stock in RPMI 1640 (Cat #11875, Life Technologies, NY, USA) supplemented with 10% FBS. Cells were cultured in T75 flasks (CellStar) and were maintained at 5% CO_2 in a humidified incubator at 37^0C. Cells were passaged when at 80% confluence after washing once with 1X PBS; they were detached with 0.25% Trypsin-EDTA (Cat #15400 Gibco/Invitrogen, 0.53mM EDTA- 4Na) for 4-5 minutes and the trypsin was then deactivated with RPMI 1640 medium containing FBS. Cells were collected and centrifuged at 4000 rpm for 5 minutes (Centrifuge 5810 R G18.0). Medium was aspirated and fresh medium was added to the cell pellet. Cells were suspended in the media and 1 ml of cell suspension was added in T75 flask with 10ml RPMI 1640 medium. Cells were plated and allowed to adhere to the plate overnight under incubation. All plates with cells were examined for bacterial and fungal infections prior to experiments. Experiments were performed within 10-12 passages of cells from frozen stock. Cells were discarded after 12 passages and a new frozen vial was thawed.

2.3 Cellular growth suppression assay for single drugs

NSCLC cells were seeded at a density of 20,000 cells/well in a 12-well plate in RPMI 1640 media supplemented with 10% FBS and allowed to adhere for 48 hours. This time point was defined as T_0 h. Conditions were plated in duplicate. Fresh media containing graded concentrations of drugs were added after 48 hours. Whenever PTX was used in the treatment, the medium used was RPMI 1640 supplemented with 10% dFBS. Experiments typically lasted for 72 hours after drug treatment. Following the incubation period, cells were washed with 1X PBS, trypsinized in 1.5 ml 1x trypsin-EDTA, and 1 ml of a single-cell suspension was counted electronically using a Z1 Coulter Particle Counter (Figure 3; Beckman Coulter, Brea, CA). Data were analyzed using Microsoft Excel 2010 (Microsoft Inc.,

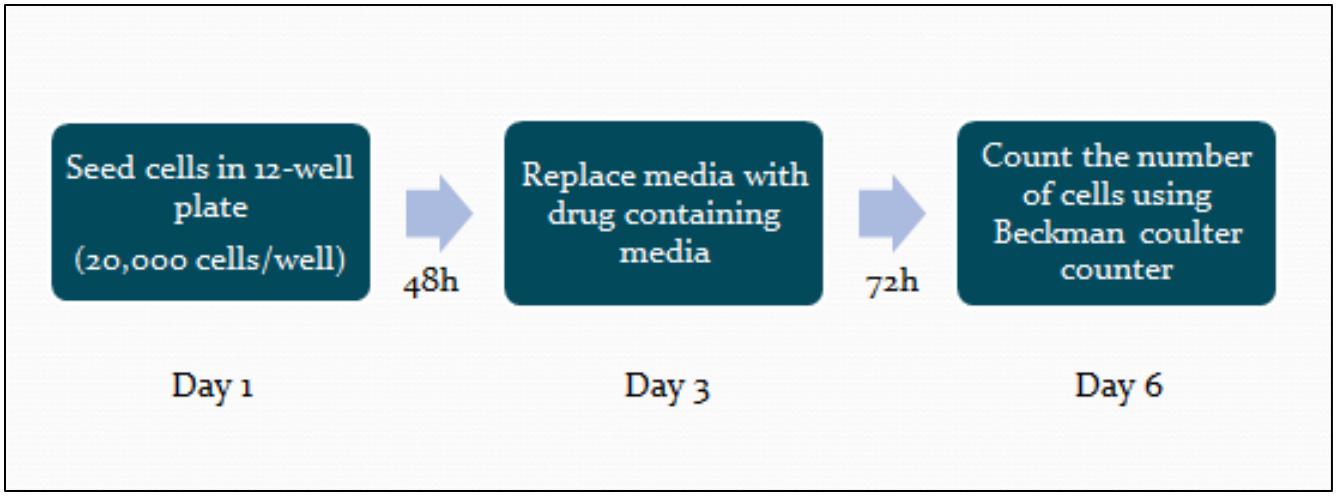

Figure 5: Schematic representation of cellular growth suppression assays in a 12-well plate.

Cells were seeded in 12-well plates at a density of 20000 cells per well. After allowing cells to adhere for 48 hours, media was replaced with fresh media containing indicated drugs. After 72 hours following drug treatment, media was aspirated and cells were counted using a Beckman Coulter counter.

Redmond, WA), and SigmaPlot version 12.3 software (Systat Software Inc, San Jose, CA). Data is presented as percent cell growth of experimental samples relative to controls in the absence of drug. Data are expressed as the mean ± SD.

2.4 Cellular growth suppression assay for combinations of drugs: Design and treatment

H358 cells were plated and allowed to adhere as mentioned in section 2.3. Fresh media containing graded concentrations of single drugs (Drug A, Drug B) and combination of two drugs (Drugs A+B) were added after 48 hours (T_0 h), as discussed below. The rest of the experimental protocol and analysis was done as in section 2.3.

The combination drug treatment protocol was as follows:

In order to study the combined effects of two drugs, data were needed from individual drug treatment at the same time as the combination treatment was performed. Hence, in every combination study, individual drug dose-response was also conducted as in section 2.3. For the combination treatment wells, the following experimental design was used (also see Figure 6).

Drug A: graded concentrations (e.g.: PTX = 0, 10, 32, 100, 320, 1000, 3000, 10000 nM)

Drug B: graded concentrations (e.g.: AZD8055 = 0, 10, 32, 64, 100, 320, 1000 nM)

Fresh media containing drug A was put on the cells followed by addition of drug B solution immediately.

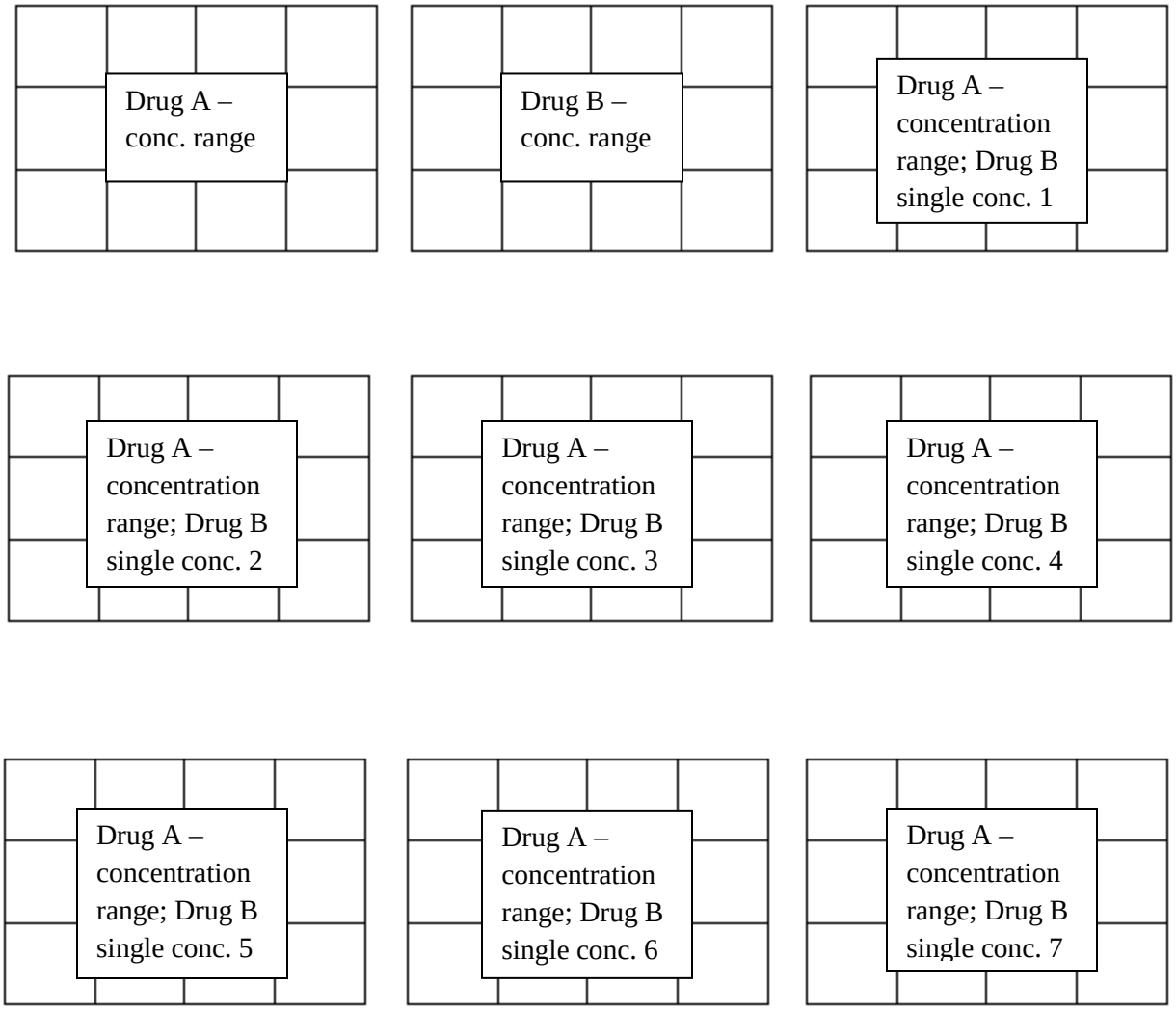

Figure 6: Design of combination drug experiments in a 12-well plate.

2.5 Evaluation of combined effects

Data obtained from the combination experiments were analyzed using Microsoft Excel 2010 (Microsoft, Redmond, WA), and SigmaPlot version 12.3 software (Systat Software Inc, San Jose, CA). Each combination dose range was plotted as a single curve on a multiple line graph to measure the shift in the dose-response curve. Data is presented as percent cell growth of experimental samples relative to controls in the absence of drug.

2.5.1 TC Chou method for calculation of IC50 and combination index

CI is a quantitative measure of the degree of drug interaction in terms of synergism (CI < 1), additive effect (CI = 1), or antagonism (CI > 1) for a given combination treatment. Inhibitory concentration 50 (IC_{50}) and Combination Indices (CIs) were calculated using CompuSyn software program (ComboSyn, Inc., Paramus, NJ, USA). Affected fraction (Fa) is defined as a function of effect level (e.g., degree of inhibition) by a dose of drug. Fa values were calculated according to the program's instruction as follows: [(100 - % growth value)/100] (Chou 2010).

2.5.2 Isobolograms

An isobologram is a graphical representation of drug interactions and is considered as a "gold standard" for the assessment of drug combinations (Chou 2010). The construction of isobolograms was done using normalized IC_{50} values of compound A alone and in the presence of graded concentrations of compound B, and normalized IC_{50} values of compound B alone and in the presence of graded concentrations of compound A. The fractional values of the individual IC_{50} of compound A and B needed to affect a 50% inhibition were then plotted on the x and y axes respectively. A typical isobologram consists of a line of additivity, which is a line joining the IC_{50}s of both the compounds on x and y axes. If the combination drugs data falls on the line of additivity, the drug interaction is called additive. If the data lies above or below the line of additivity, the drug interaction is called antagonistic or synergistic, respectively. A

typical isobologram can be interpreted as follows:

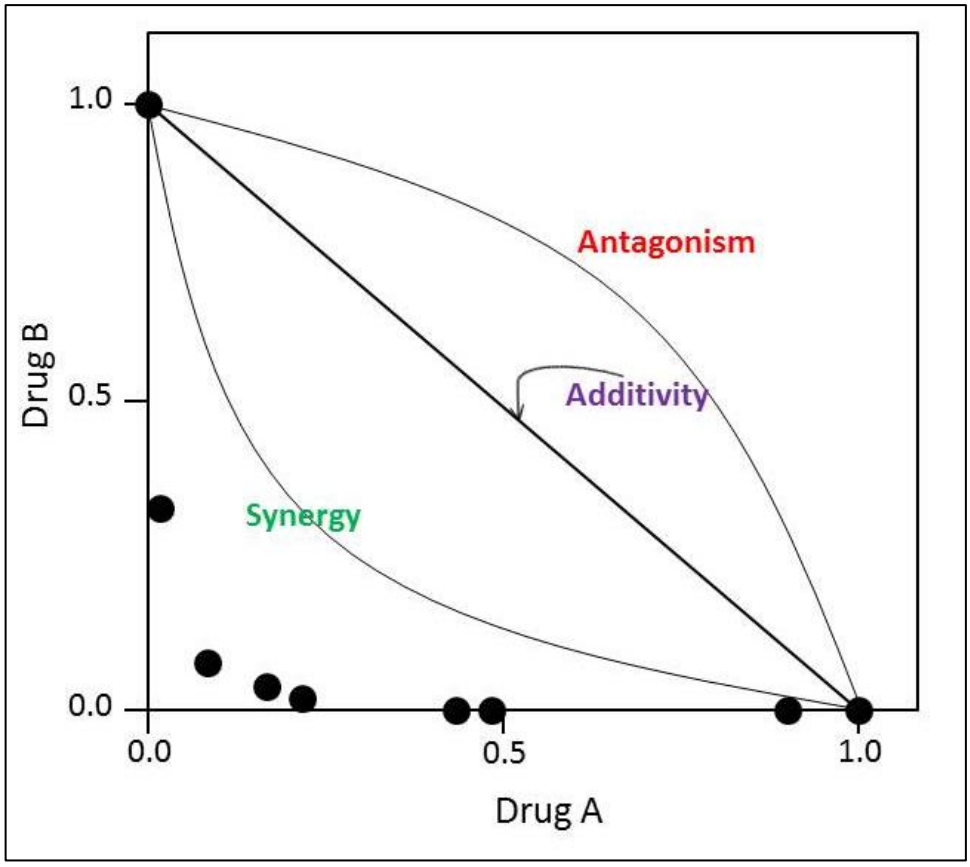

Figure 7: A schematic representation of an isobologram.

2.6 Immunoblotting

Total Protein Isolation: Protein was typically harvested from 2-5 x 10^6 cells grown on 100 mm dishes (CytoOne). Prior to total protein harvest, one protease inhibitor cocktail tablet was dissolved in 25 ml 1X PBS and placed on ice. Tissue culture plates were kept cold throughout the harvesting procedure. Cells were washed once with 1.5 ml cold PBS (containing protease inhibitor), scraped, and collected by centrifugation in pre-weighed 1.5 ml centrifuge tubes at 1,000 rpm for 5 minutes at 4°C. The supernatant fluid was aspirated and then pelleted cells were lysed in cold buffer containing 62.5 mM Tris-HCl pH 6.5, 2% SDS, 5% glycerol, 5% 2-mercaptoethanol, 50 mM NaF, and a 1X concentration of Complete EDTA-free Protease Inhibitor Cocktail. Lysates were sonicated on high power for 7.5 minutes at 30 seconds on, 30 seconds off intervals in a Diagenode Bioruptor bath sonicator and then were centrifuged at 14,000 rpm for 5 minutes.

Protein Concentration Assays: The Bradford Assay was used to determine protein concentration of each sample using the Bradford Reagent according to the manufacturer's protocol with BSA as a standard. Duplicate assays were conducted for each sample as well as for the standard curve. Standard curve samples contained 699-799µl of H_2O at 20µl intervals, 1µl of SDS lysis buffer and BSA (0-10µg) while sample tubes contained 799µl of H_2O and 1µl of protein extract. Bio-Rad dye concentrate (Cat # 500-0006) (200µl) was added to each tube. After 15 minutes incubation at room temperature, absorbance was determined using a spectrophotometer at 595nm wavelength. Typically, protein concentrations were 2-5 µg/µl. Protein was placed in single-use aliquots and stored at -80°C.

SDS-PAGE and Protein Transfer: Gel electrophoresis and wet membrane transfers were performed using the Mini PROTEAN-3 Cell system (Cat #1653301) from Bio-Rad Laboratories. Total protein was mixed with an equal volume of Laemmli Sample Buffer, boiled for 5 minutes, and 20 µg was loaded onto 1.5 mm SDS-polyacrylamide gels, poured according to the recipe provided with 30% Acrylamide/Bis 37:5:1 (Cat #1610158) from Bio-Rad Laboratories. An aliquot (5-10 µl) of Dual Color Precision Plus

Protein Standard was also loaded onto every gel for mass determination. Typically, protein was resolved on 7.5% or 12% gels in running buffer (25 mM Tris base, 250 mM glycine, 0.1% SDS) at 50 volts for 30 minutes (or until protein migrated out of the stacking gel) followed by 120 volts for 1-1.5 hours to optimally separate the proteins of interest.

After electrophoresis, the gel was washed in water then transferred to a PVDF membrane that was pre-washed in 100% methanol. Transfer was performed in ice bath with stir bar placed in transfer apparatus for 60 minutes at 100 volts in 1X Transfer Buffer (25mM Tris-HCl, pH 8.3, 192mM glycine, 10% methanol and 0.04% SDS). Following the transfer, membranes were dipped in methanol and dried on the lab bench for 15 minutes before being immunoblotted.

Antibody Detection: A general antibody detection procedure is described in this section. For detailed conditions for each antibody, refer to Table 1. Dried membranes were soaked briefly in methanol and non-specific proteins were blocked for 1 hour in either StartingBlock Blocking Buffer. Membranes were washed three times for 5 minutes in 0.1% TBS-T (25mM Tris-HCl, pH 8.3, 192mM glycine, 0.04% SDS, 0.1% Tween-20). Primary antibodies diluted in StartingBlock Buffer were incubated on the membranes overnight at 4°C with rotation in sealed plastic containers to minimize antibody consumption. Membranes were washed 3 times with 0.1% TBS-T for 5 minutes and incubated for 1 hour in horseradish peroxidase-conjugated secondary antibody. After incubation, three 10 minute washes in 1X TBS-T were performed. It was found that washing more stringently during this step greatly diminished non-specific background during exposure. Membranes were incubated with West Pico (Pierce, Cat# 34080) or West Dura SuperSignal chemiluminescence substrate (Pierce, Cat# 34075) for 5 minutes. Blots were developed using ODYSSEY LI-COR imager (LI-COR Biosciences, Nebraska, USA) using 700 nm and chemiluminescence channels. If the chemiluminescent conditions were not known, West Pico was applied first. If no signal was apparent, the blot was rinsed with 0.1% TBS-T, and West Dura solution was applied. Signal was usually observed with one of these conditions, and rarely was a more stringent detection reagent applied.

Table 1: List of antibodies used for western blotting

Antigen	Primary Ab obtained from	Primary Ab Dilution	Blocking Buffer	Secondary Ab Used	Secondary Ab Dilution	Expected protein band size	Chemiluminescent substrate prepared
p70-S6K1	Cell Signaling Cat. 9202S	1:1000	Starting Block	Goat Anti-Rabbit	1:5000	70 kD	Dura
P – p70-S6K1	Cell Signaling Cat. 9205L	1:500	Starting Block	Goat Anti-Rabbit	1:5000	70 kD	Dura
4E-BP1(53H11)	Cell Signaling Cat. 9644P	1:1000	Starting Block	Goat Anti-Rabbit	1:5000	15-20 kD	Pico
P-4E-BP1(T37/46)	Cell Signaling Cat. 2855L	1:1000	Starting Block	Goat Anti-Rabbit	1:5000	15-20 kD	Dura
eIF4E (C4SH6)	Cell Signaling Cat. 2067S	1:1000	Starting Block	Goat Anti-Rabbit	1:5000	70 kD	Dura
β - Actin	Cell Signaling Cat. 3700S	1:5000	Starting Block	Goat Anti-Mouse	1:5000	42 kD	Pico

2.7 m7GTP capture of 4E-BP1-eIF4E complexes

Following the indicated drug treatments, cells were lysed on ice for 30 minutes in IP buffer [25 mmol/L of HEPES (pH 7.5), 1% NP40, 100 mmol/L NaCl, 1 mmol/L EDTA, 1 mmol/L EGTA, 50 mmol/L NaF, 1 mmol/L phenylmethylsulfonylfluoride, 0.1% 2-mercaptoethanol, and 1X Roche Complete Protease Inhibitor Tablet]. An aliquot (500 mg) of cleared lysate was incubated with 40 mL of 50% slurry of m7GTP-Sepharose (GE Lifesciences) for 2 hours at 4°C with rotation. m7GTP captured complexes were washed with IP buffer 4 times, resuspended in Laemmli sample buffer, and boiled for 5 minutes before being resolved on a 12.5% SDS-PAGE gel and immunoblotted as described above.

Chapter 3: Results

3.1 Pemetrexed and AICAR inhibit the proliferation of human NSCLC cells

As mentioned in section 1.2, Ding et al (2008) have shown that tumor suppressor genes p53, CDKN2A and STK11, and several oncogenes KRAS and EGFR are most frequently mutated in lung cancers. We examined the anti-proliferative effects of the AMPK activators, PTX and AICAR, in three NSCLC cell lines that differ in the mutational status of the KRAS and/or p53 genes. The cell lines were H661, which had a mutation in p53 and p16 genes, H441, which had a mutation in p53 and KRAS genes, and H358, in which the p53 gene was lost and the KRAS gene was mutated. The specific genotype of each cell line can be found in Table 2. Each of these cell lines was plated in 12-well plates (3.9 cm^2/well), allowed to adhere over 48 hours, and then continuously exposed to increasing concentrations of drug over 72 hours. Cell growth was plotted as a percent of control growth. Following PTX or AICAR treatment, the cell growth rate was suppressed in all three cell lines in a dose-dependent manner (Figure 8 and Figure 9). H661 and H358 were equi-sensitive to AICAR and H441 was, on the average, 3-fold less sensitive. Complete suppression of cell growth required AICAR concentrations $\geq$ 1 mM. The cell lines that differed dramatically in genotype (Table 3) demonstrated minimal difference in sensitivity to AICAR. On the other hand, H441 and H358 exhibited equal sensitivity to PTX and the growth of these cell lines was suppressed at lower concentrations than the H661 cell line. Although, H661 showed dose-dependent growth inhibition, the effect plateaued off at high doses of PTX. PTX was substantially more potent than AICAR with IC50 values 100-1000 times lower for these cell lines. H441 and H358 cells have mutations (or deletions) in both the p53 and KRAS genes. H661, in addition to a mutation in p53, has a mutation in the p16 gene (also known as CDKN2A), which is a tumor suppressor gene plays an important role in cell cycle regulation (Stone et al. 1995) (see discussion). Interestingly, a recent publication reported that NSCLC cell lines with mutant KRAS gene were, as a class, measurably more sensitive to PTX than NSCLC lines with wild type

Table 2: Partial genotype of the NSCLC cell lines used in these studies.

Genes / Cell line	p53	KRAS	p16
H661	R158L	wt	C457+1G>T
H441	R158L	G12V	wt
H358	null	G12C	wt

- Mutation status of p53, KRAS, and p16 in each cell line was determined from the Sanger Catalogue of Somatic Mutations in Cancer database (COSMIC; http://www.sanger.ac.uk/genetics/CGP/cosmic)

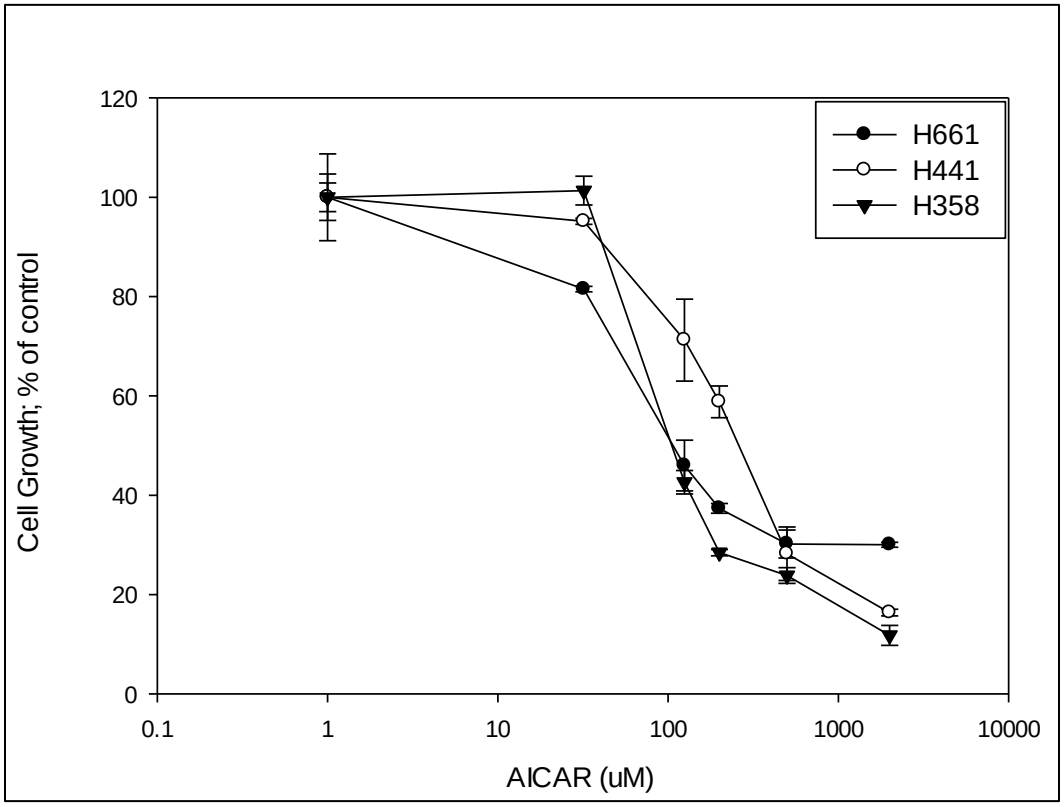

Figure 8: Growth suppression of NSCLC cells in the presence of AMPK activators AICAR (A) and pemetrexed (B). Cells were treated with indicated drugs for 72 hours and the number of cells per well was measured using a Beckman Coulter counter.

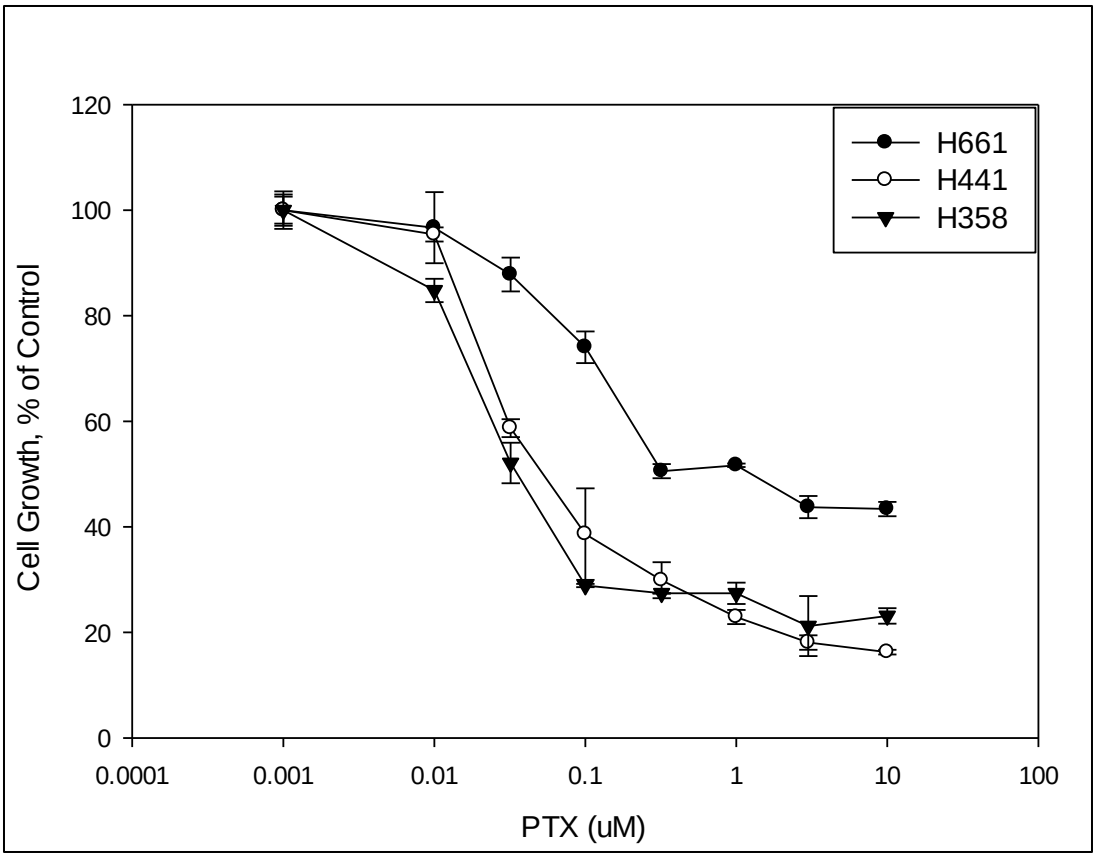

Figure 9: Growth suppression of NSCLC cells in the presence of AMPK activators AICAR (A) and pemetrexed (B). Cells were treated with indicated drugs for 72 hours and the number of cells per well was measured using a Beckman Coulter counter.

KRAS (Moran et al. 2014). These experiments demonstrated that PTX and AICAR dose-dependently inhibited the growth of NSCLC cells in vitro.

3.2 NSCLC cells showed differential sensitivity to PTX in the presence and absence of thymidine

The primary target of PTX and its metabolites was originally shown to be thymidylate synthase (TS; Taylor et al. 1992, Hsieh et al. 1998). Recently, it was discovered in our laboratory that PTX also acts on a secondary target AICART, the second folate dependent enzyme of de novo purine synthesis (Racanelli et al. 2009, Rothbart et al. 2010). The inhibition of purine synthesis resulted in the accumulation of ZMP which, in turn, causes a marked activation of AMPK (Racanelli et al. 2009, Rothbart et al. 2010). To separate the effects of these two mechanisms of PTX, we circumvented the action of PTX on TS to allow us to study its effect only on AMPK activation. Hence, we performed growth inhibition assays with PTX in the presence and absence of 5.6 μmol/L thymidine, a salvageable source of thymidylate that reverses the effects of TS inhibition by PTX. As expected, PTX in the absence of thymidine, the condition that displays the growth inhibitory effect of both TS and AICART, was much potent than in the presence of thymidine, which reflects only AICART inhibition. The H441 cell line, in which p53 and KRAS are both mutated, showed the highest difference in sensitivity for PTX with and without thymidine, with a 40-fold decrease in IC_{50} in the absence of thymidine. A marked difference in sensitivity for PTX with and without the addition of thymidine was also observed with H358 cell line (p53 null, KRAS mutant) with approximately 10-fold decrease in IC_{50} of PTX when thymidine was not added to the media. H661, in which KRAS was wild type showed the least difference in sensitivity for PTX – alone or with thymidine, and we were unable to obtain IC_{50} values in the presence of thymidine even at very high concentration (10 μM) of PTX used. We concluded that the H661 cell line was relatively refractory to PTX. These experiments did not shed any light on why the response of these cell lines to PTX was so markedly

(A)

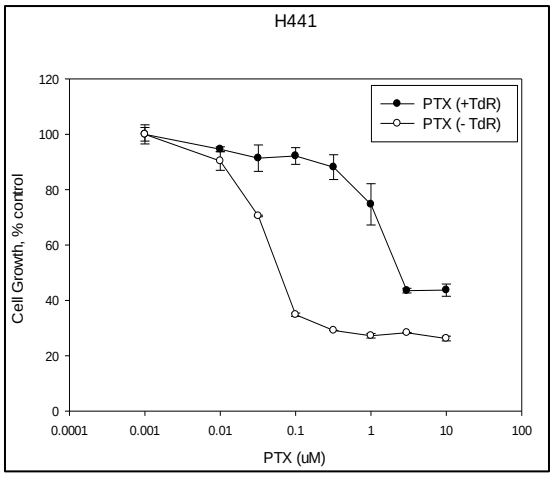

(B)

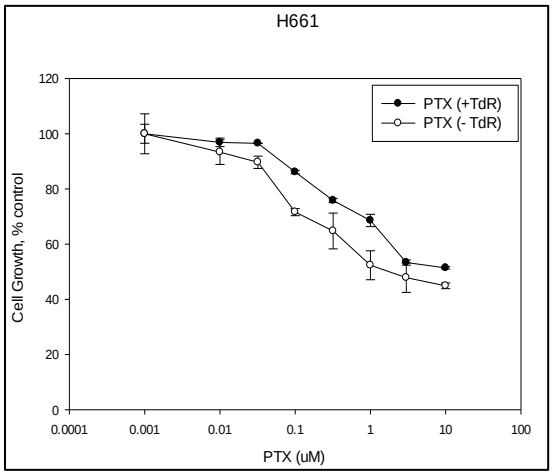

(C)

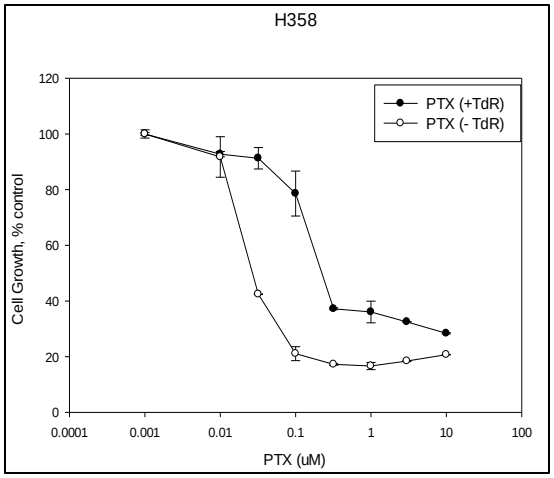

Figure 10:Growth suppression effects of PTX in the presence and absence of Thymidine on NSCLC cell lines A)H441, B)H661 and C)H358. NSCLC cells were treated PTX, in the presence and absence of thymidine for 72 hours and the number of cells per well was measured using a Beckman Coulter counter.

different. Whether the existence of a p16 mutation in this cell line was involved was interesting to consider, but more studies are required to understand these effects.

3.3 Inhibition of mTORC1 and mTORC2 is more detrimental to cell growth and proliferation than inhibition of mTORC1 alone

Rapamycin was the first drug discovered to inhibit the mammalian target of rapamycin (mTOR) protein. The rapamycin analog, RAD001 acts by the same molecular mechanism as rapamycin to allosterically inhibit mTORC1 and is currently approved for the treatment of renal cell carcinoma. We evaluated the efficacy of RAD001 as an inhibitor of cell growth in NSCLC cell lines. It was observed that RAD001 did decrease cell growth but that the dose response curves were extremely shallow (Figure 11). This came across as an interesting fact as previous studies have shown that RAD001 at concentrations of 5-20 nM completely inhibit mTORC1 activity. RAD001 is used clinically for the treatment of renal cancer and plasma concentrations only reach 5 – 20 nM. Yet, even at a 100-fold (2000 nM) greater concentration than what is used clinically, it was not possible to obtain an IC_{50} value in the H661 and h441 cells suggesting that RAD001 would be a poor drug to inhibit proliferation of NSCLC cells with these genotypes. RAD001 is directed towards only mTORC1 inhibition without any effect on mTORC2 and also results in release of feedback control of Akt activity. This may suggest that the reduced efficacy of RAD001 is due to an incomplete block of mTOR signaling and hence, cell growth. In order to overcome this problem and inhibit mTORC2 mediated feedback loops that reduce the efficacy of rapalogs, we used a dual mTORC1/2 inhibitor AZD8055 (Figure 12). AZD8055 demonstrated greater efficacy and potency over RAD001 in suppressing growth of cells. All three NSCLC cell lines were equi-sensitive to AZD8055 and exhibited IC_{50}s in the range of 80 – 120 nM. This comparison furnishes direct evidence that inhibition of both mTORC1 and mTORC2 is more beneficial in controlling cell survival and growth than is inhibition of mTORC1 alone.

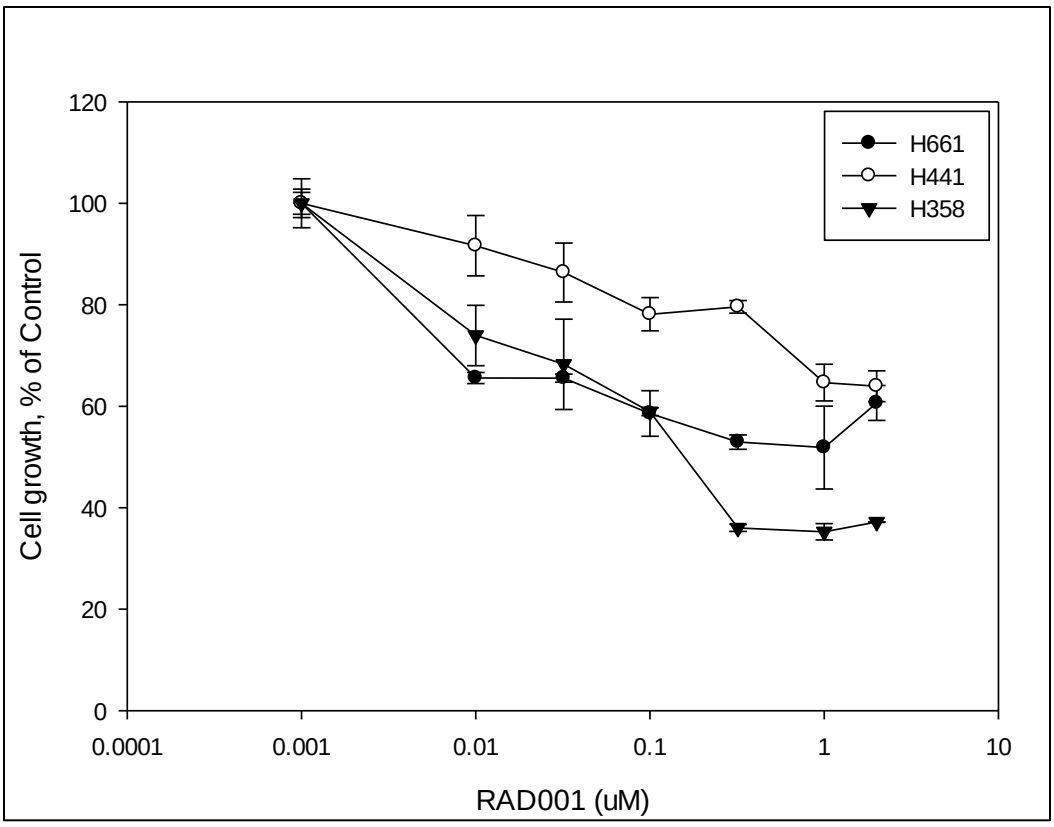

Figure 11: Growth suppression of NSCLC cells in the presence of mTORC1 inhibitor RAD001. Cells were treated with indicated drugs for 72 hours and the number of cells per well was measured using a Beckman Coulter counter.

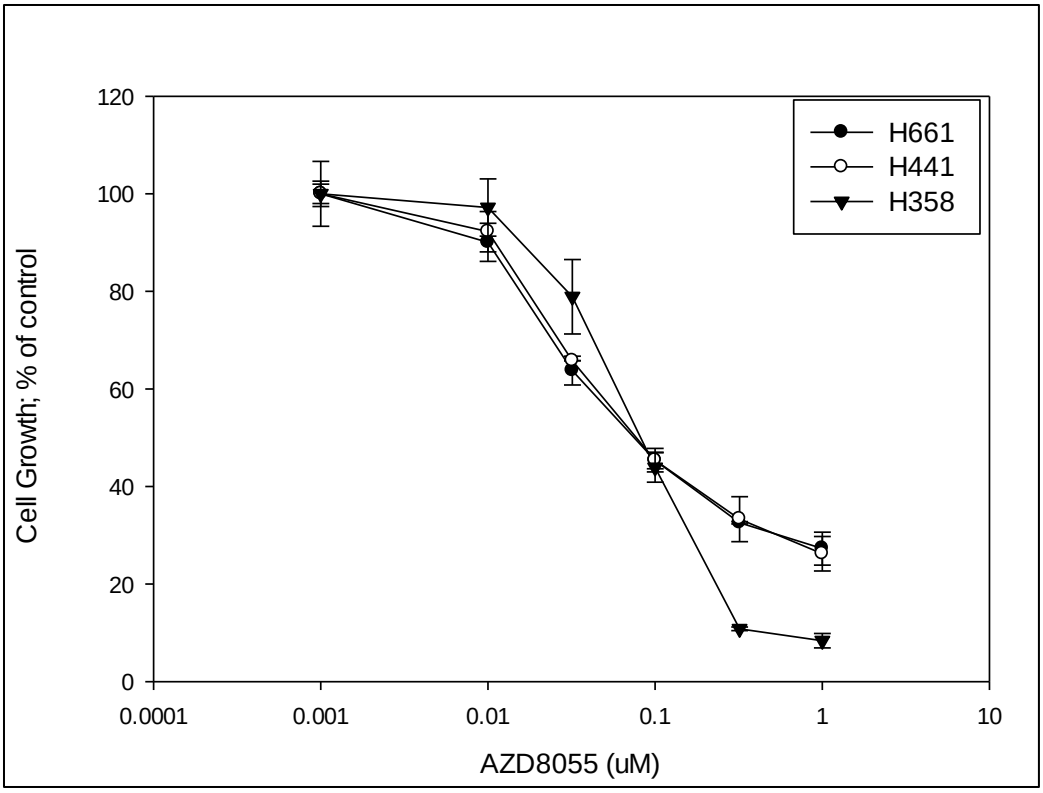

Figure 12: Growth suppression of NSCLC cells in the presence of dual mTORC1/2 inhibitor AZD8055. Cells were treated with indicated drugs for 72 hours and the number of cells per well was measured using a Beckman Coulter counter.

3.4 Combination of AZD8055 with AMPK activators AICAR and Pemetrexed showed superior anti-proliferative effects than either drug alone

3.4.1 AICAR enhances the effects of AZD8055 and vice-versa

We demonstrated that both AICAR and PTX were able to suppress the growth of NSCLC cells. In addition, AZD8055 was superior to RAD001 in terms of growth inhibitory effects. Hence, we tested the effects of combination of AICAR or PTX with AZD8055 on cell growth and proliferation. Because the H358 cell line has shown intermediate differences in sensitivity to PTX in the presence and absence of thymidine and grew reproducibly well in culture, we decided to perform detailed drug interaction studies on this cell line. The main aim of this project is to evaluate combinations of mTOR antagonists and PTX; hence, using a cell line that shows intermediate differential sensitivity to PTX indicated the most representative sensitivity of the two targets of this drug, namely TS and AMPK. On combining AICAR and AZD8055, we saw that the dose-response curve of one drug was not shifted to the left with the addition of lower increments of the other drug, but at concentrations on the range of an IC_{50} of one drug, the dose-response curve was substantially shifted (Figure 13). The IC_{50} of AICAR was reduced by approximately 5-fold with the addition of 64 nM AZD8055. Similarly, the addition of 100 μM AICAR reduced the IC_{50} of AZD8055 by 10-fold. This suggested that addition of an AMPK activator enhanced the growth inhibitory effects of an mTOR inhibitor and vice-versa. Thus, these data were analyzed for fractional IC_{50} and plotted as an isobologram (Figure 14). This analysis indicated an additive combined effect on tumor cell growth.

3.4.2 Pemetrexed enhances the effects of AZD8055 and vice-versa

Following the effects seen with combinations of AICAR and AZD8055, we performed a similar experiment with AZD8055 and an US FDA approved drug for NSCLC, pemetrexed. In order to reverse the effects of PTX on TS, this experiment was carried out in the presence of 5.6 μM thymidine. As also

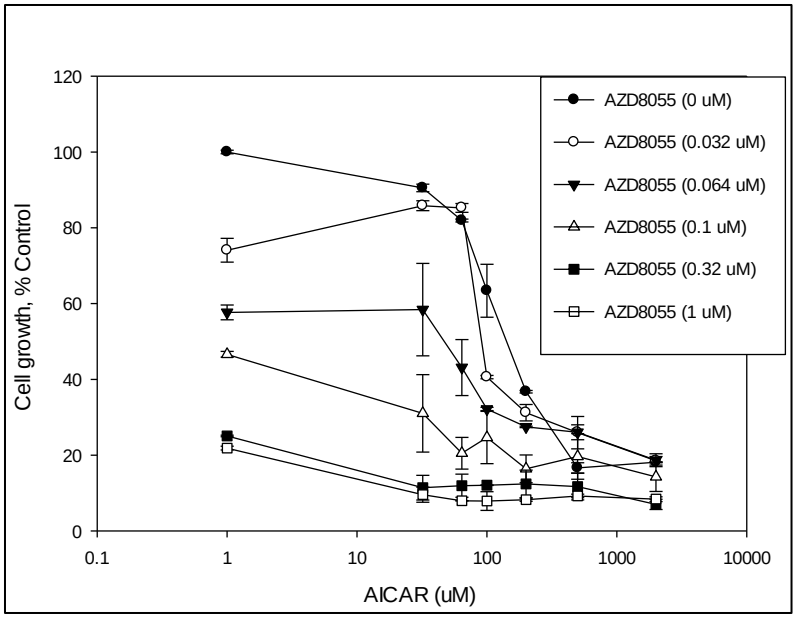

(A)

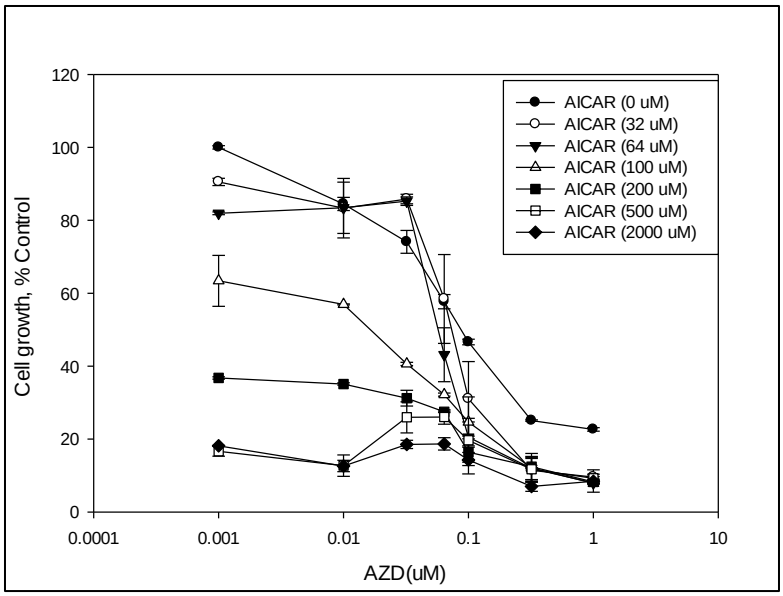

(B)

Figure 13: Enhancement of growth suppression effects of AICAR in combination with AZD8055 and vice-versa. Leftward shifts in the IC_{50} in the Concentration-Effect curves of A) AICAR in the presence of AZD8055 dose increments and B) AZD8055 in the presence of AICAR dose increments.

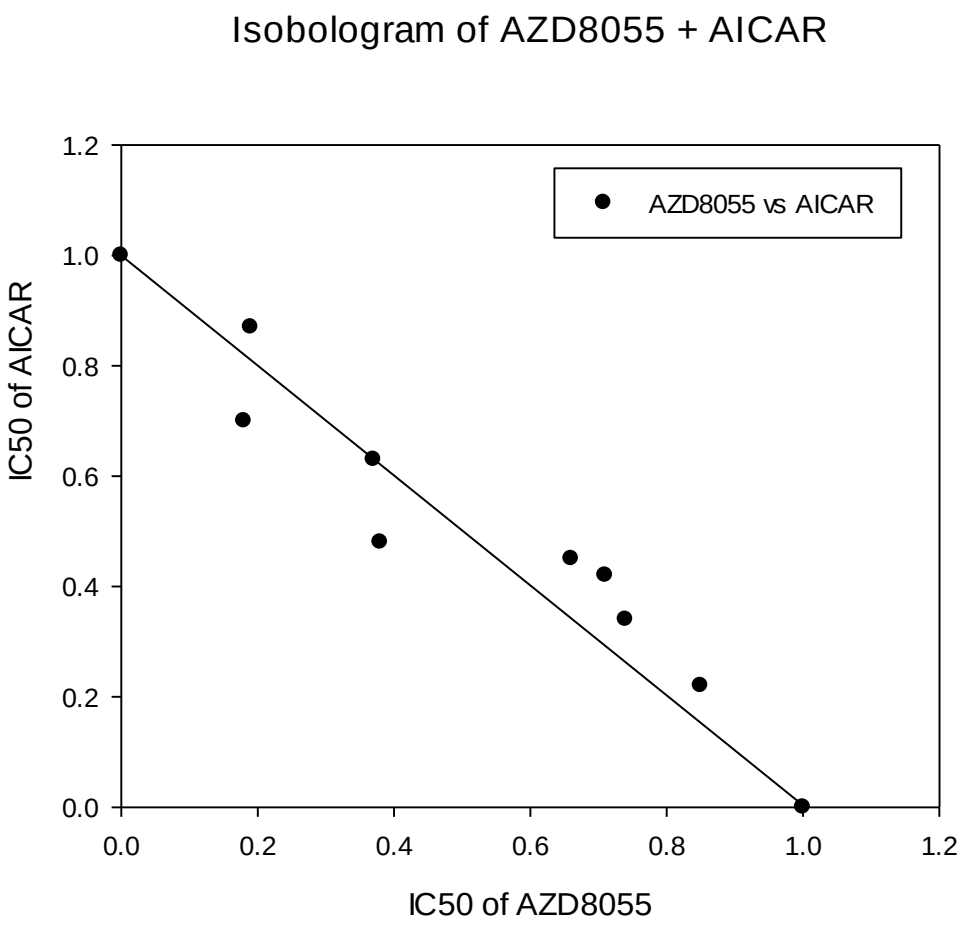

Figure 14: Isobologram of additivity for AICAR+AZD8055. The combination of AICAR+AZD8055 was found to be additive, when normalized data points from the growth suppression assay of AICAR+AZD8055 were plotted on the isobologram.

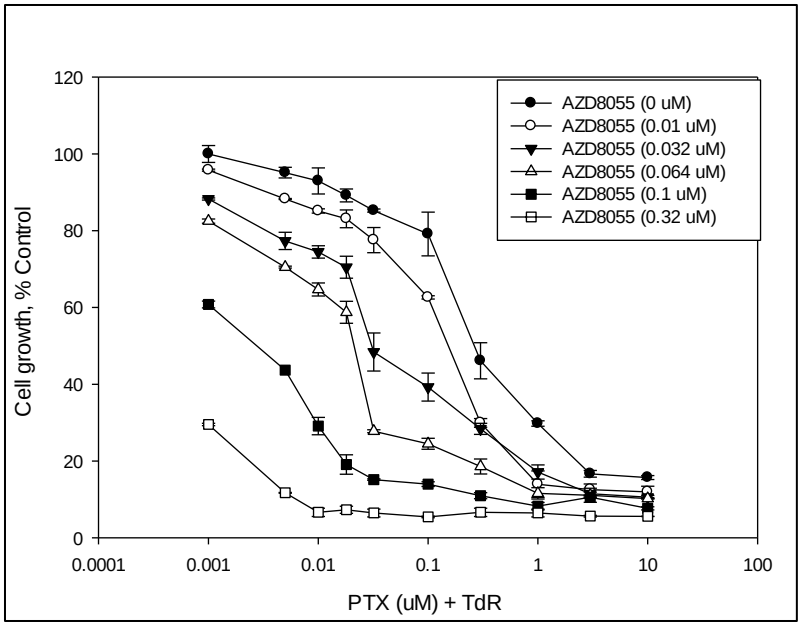

(A)

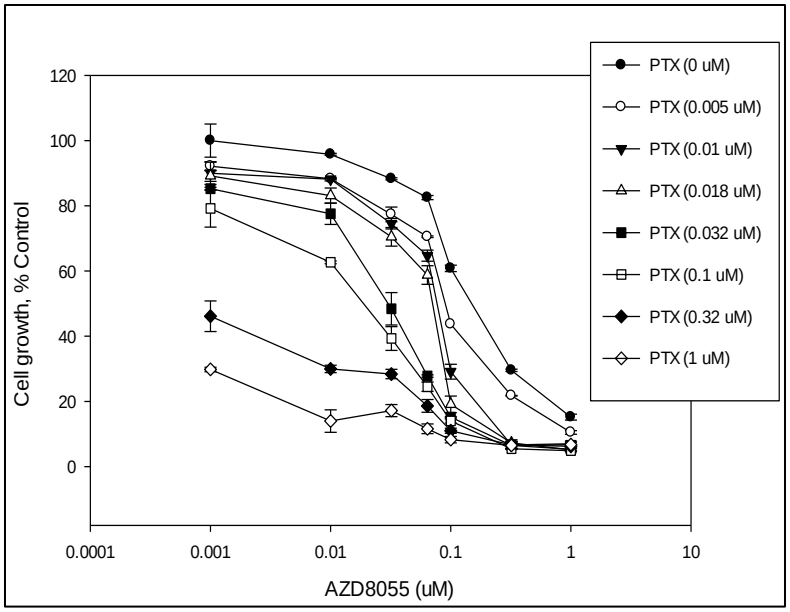

(B)

Figure 15: Enhancement of growth suppression effects of pemetrexed in the presence of thymidine, in combination with AZD8055 and vice-versa. Leftward shifts in the IC_{50} in the Concentration-Effect curves of A) PTX in the presence of AZD8055 dose increments and B) AZD8055 in the presence of PTX dose increments.

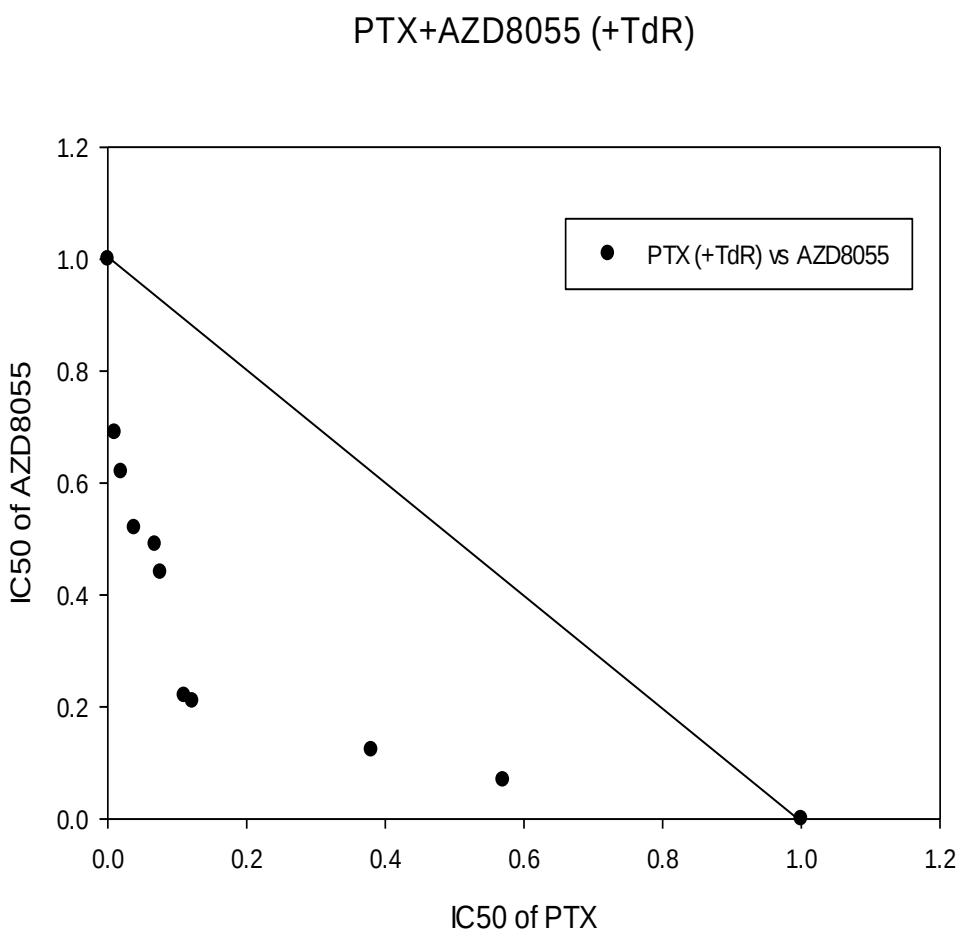

Figure 16: Isobologram of additivity for PTX+AZD8055, in the presence of thymidine. The combination of PTX+AZD8055 in the presence of thymidine was found to be highly synergistic, when normalized data points from the growth suppression assay of PTX+AZD8055 (+ thymidine) were plotted on the isobologram.

seen in figure 10, we observed that PTX by itself showed a dose-dependent decrease in cell growth of H358 cells in the presence of thymidine at an IC_{50} of ~ 300 nM. The addition of a small amount (10 nM) of the catalytic site mTORC1/2 inhibitor reduced the IC_{50} to ~ 200 nM, with a further decrease in IC_{50} of PTX seen with addition of 32 nM AZD8055 (Figure 15A). This reduction in IC_{50} was approximately 8-10 folds, which is very promising in terms of cancer therapeutics. Further addition of AZD8055 to PTX reduced the IC_{50} even more, suggesting that AZD8055 enhanced the effects of PTX in inhibiting growth and proliferation of H358 cells. When the data was plotted in the reverse manner to evaluate the benefit of adding PTX to AZD8055, we observed a similar phenomenon. AZD8055 by itself suppressed growth of cells very efficiently at an IC_{50} of ~ 120 nM. However, addition of small increments of PTX progressively shifted the dose- response curve of AZD8055 to the left (Figure 15B), demonstrating a reduction in the IC_{50} of AZD8055 and suggesting that each drug enhanced the growth inhibitory effects of other when co-administered. The isobologram constructed to summarize this combination indicated a strongly synergistic interaction (Figure 16).

3.4.3 Pemetrexed combined with AZD8055 results in enhanced antitumor efficacy in the absence of thymidine

To determine the utility of PTX and AZD8055 combination in clinically relevant conditions, we performed the aforementioned combination experiment of PTX and AZD8055 without adding 5.6 µM thymidine to the media. Under such conditions, PTX acts as an inhibitor of AICART, as an activator of AMPK, as well as an inhibitor of TS and is more substantially potent than in the presence of thymidine, when it is an AICART inhibitor and activator of AMPK alone. In the absence of thymidine, PTX demonstrated more than a 5-fold greater potency at suppressing growth of H358 cells than that in the presence of thymidine (Figure 10). The IC_{50} observed for PTX by itself was approximately 32 nM with a sharp dose- response curve (Figure 17A). In addition to the superior potency observed of PTX by itself, addition of AZD8055 to PTX further shifted the IC_{50} of PTX towards the left indicating that addition of a

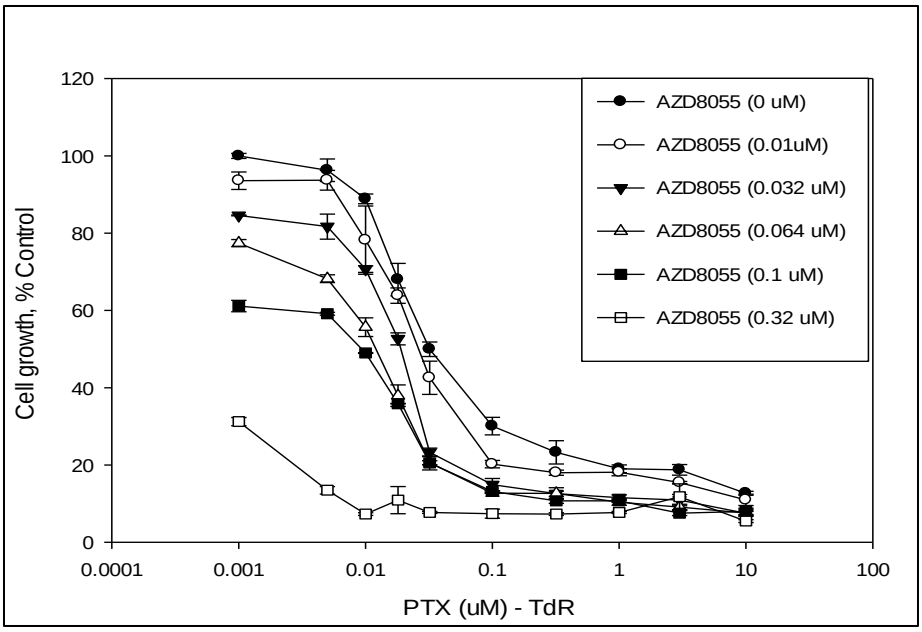

(A)

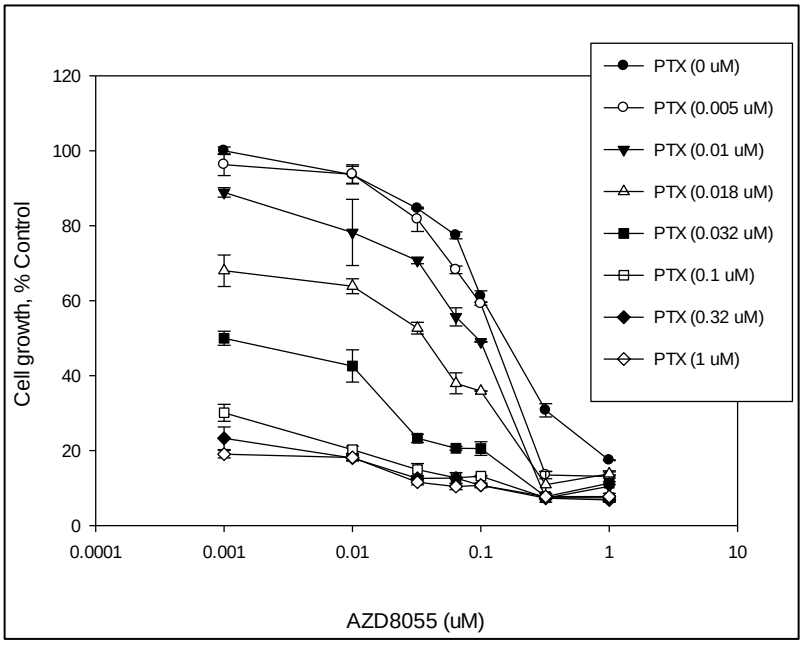

(B)

Figure 17: Enhancement of growth suppression effects of pemetrexed in the absence of thymidine, in combination with AZD8055 and vice-versa. Leftward shifts in the IC_{50} in the Concentration-Effect curves of A) PTX in the presence of AZD8055 dose increments and B) AZD8055 in the presence of PTX dose increments.

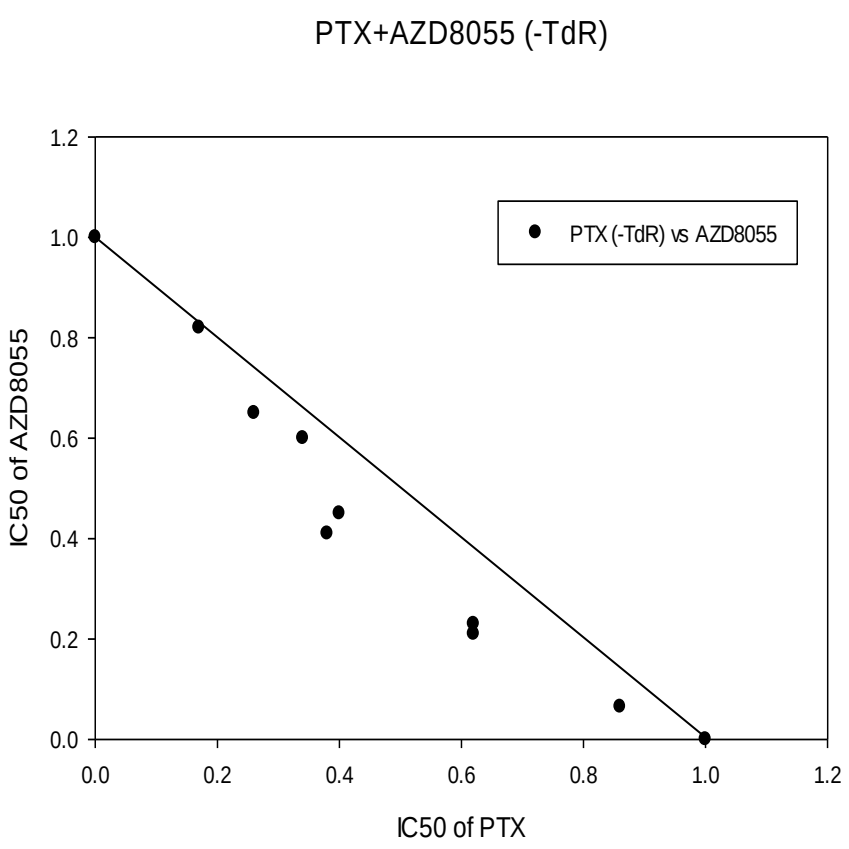

Figure 18: Isobologram of additivity for PTX+AZD8055, in the absence of thymidine. The combination of PTX+AZD8055 was found to be mildly synergistic to additive, when normalized data points from the growth suppression assay of PTX+AZD8055 were plotted on the isobologram.

Table 3: IC_{50} concentrations of H358, H441 and H661 for PTX, AICAR, AZD8055 and RAD001.

IC50 values (μM)			
Treatment	H358	H661	H441
AICAR	139; 100; 120; 90	139	320
PTX +Tdr	0.29, 0.2; 0.3; 0.32	> 2	2
PTX -Tdr	0.03, 0.029, 0.03, 0.039	> 2	0.04, 0.05, 0.007
AZD8055	0.09; 0.08; 0.2; 0.09	0.13	0.11
RAD001	> 1 , > 1	> 3, > 3	> 3, > 3

direct mTOR inhibitor with PTX treatment has even greater benefits in reducing tumor cell growth. Similar to what was seen in the presence of thymidine, when the same data were plotted as a function of AZD8055 dose- response, incremental additions of PTX enhanced the anti-proliferative potential of AZD8055 with significant shifts of the dose-response curves to the left (Figure 17B). The data were analyzed for fractional IC_{50} and plotted as an isobologram (Figure 18). This isobologram indicated a somewhat synergistic pattern, but significantly less than seen in the presence of thymidine. Hence, from the growth suppression studies conducted so far, it can be concluded that the combination of AMPK activators (PTX or AICAR) with ATP-site dual mTOR inhibitor AZD8055 exhibits greater anti-tumor efficacy over either monotherapy.

3.5 Dual blockade of PI3K/Akt/mTOR and LKB1/AMPK/mTOR pathway is synergistic or additive in NSCLC cell lines

An isobologram is a graphical representation of drug interactions and is considered by many investigators to be the "gold standard" for the assessment of drug combinations. In order to confirm whether any of the drug combinations we had used had anti-tumor efficacy than expected from that of the individual drugs, isobolograms were constructed using normalized IC_{50} values as described in section 2.5.2 and were examined for synergy, antagonism, and additivity in H358 cells. We observed that in the combination of AICAR and AZD8055, data points were scattered near the line of additivity on both sides and that the interaction was clearly additive in NSCLC H358 cell line (Figure 14). Upon plotting the data of Figures 15A and 15B as an isobologram (Figure 16), the combination of PTX and AZD8055 in the presence of 5.6 uM thymidine was found to be highly synergistic with all data points lying in the zone of the isobologram substantially below the line of additivity. A comparison of the isobolograms in figures 14 and 16 displays a strikingly different outcome. This was very surprising in view of the hypothesis that both PTX in the presence of thymidine and AICAR were thought to have the same mechanism, namely activation of AMPK (see Discussion). When the data points from the experiment of PTX and AZD8055 combination in the absence of thymidine (Figures 17A and 17B) were constructed into an isobologram

(Figure 18), they demonstrated a slightly synergistic to additive effect over the curve. This indicated that the interaction of PTX in the presence of thymidine, in combination with AZD8055 showed superior drug interaction as compared to PTX as a dual inhibitor of AICART and TS. We think that this might be because PTX in the absence of thymidine is potent by itself, and shows more than 5-fold lower IC_{50} than PTX plus thymidine (see Discussion).

3.6 Pemetrexed and AZD8055 both inhibit mTOR signaling

In an effort to explain the synergistic interaction observed with pemetrexed and AZD8055 on H358 cells, mTOR kinase inhibiton by pemetrexed and AZD8055 was assessed in intact H358 cells (Figure 19). Initially, phosphorylation of S6K1 was measured by western blotting. S6K1 is a direct downstream target of mTORC1 which plays a critical role in cap-dependent translation (Figure 2). Phosphorylation of S6K1 activates its kinase activity which then converts ribosomal protein S6 to its phosphorylated form, a necessary step in its recruitment of the components of the cap-dependent translational preinitiation complex. It was observed that pemetrexed decreased the phosphorylation of S6K1 at T389, in the presence and absence of thymidine, when compared to untreated cells; however, the hypophosphorylation of S6K1 was markedly greater with pemetrexed in the absence of thymidine and was thought to occur because of its effect on AICART as well as thymidylate synthase. AZD8055 is a potent inhibitor of both mTORC1 and mTORC2 and inhibited phosphorylation of S6K1 to much gretaer extent than pemetrexed.

3.7 Effects of combining pemetrexed in the presence of thymidine and AZD8055

In order to examine the effects of pemetrexed and AZD8055 in combination on mTOR inhibition, we tested them at 0.5, 1, and 2 X IC_{50} concentrations alone and in combination with the other drug. These

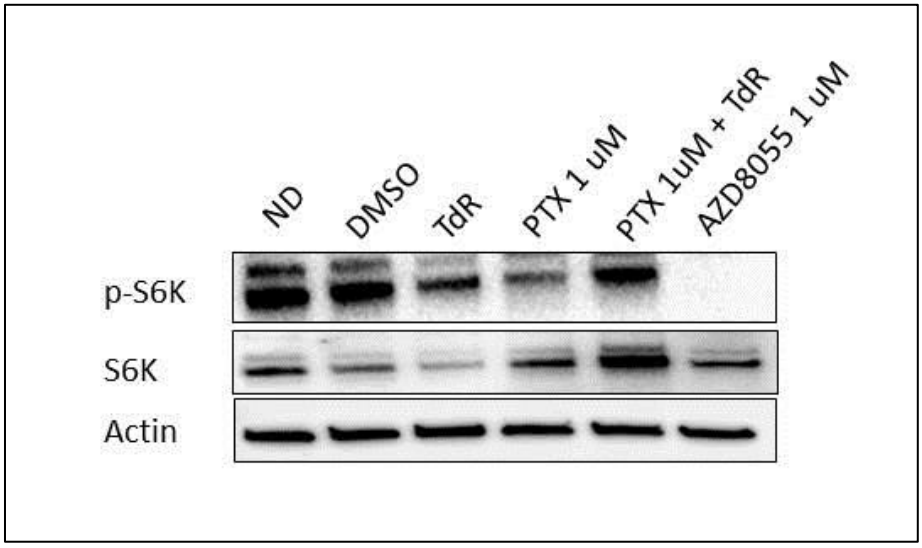

Fig 19: Effects of pemetrexed and AZD8055 on phosphorylation of S6K1 following mTORC1 inhibition.

experiments, then, tested whether the effects of these drugs on mTORC1/2 correlated with the early stages of growth inhibition and, therefore, could be said to be causative of the growth suppression. The concentrations of pemetrexed used were 160, 320, and 640 nM; and AZD8055 was used at concentrations 61.25, 125, and 250 nM. It was observed that pemetrexed (lanes 3,4, and 5; Figure 20A and 20B) dose dependently inhibited the phosphorylation of S6K1 as compared to untreated cells, with highest inhibition observed at 2X IC_{50} concentration. Pemetrexed also inhibited phosphorylation of another mTORC1 substrate 4E-BP1 dose-dependently. 4E-BP1, like S6K1, plays a critical role in cap-dependent translation. It inhibits cap-dependent mRNA translation by binding and inactivating eukaryotic translation initiation factor 4E (eIF4E) that is involved in the mRNA-ribosome binding step of eukaryotic protein synthesis. Phosphorylated 4E-BP1 by mTOR is dissociated from eIF4E, resulting in increasing protein synthesis. Thus, hypophosphorylation of 4E-BP1 by mTOR inhibition would lead to 4E-BP1 not dissociating from eIF4E resulting in inhibition of protein synthesis and cell proliferation. 4E-BP1 can be separated into hypo and hyperphosphorylated bands using a 12% gel, with the unphosphorylated form at the bottom and hyperphosphorylated forms preogressively higher in the gel. It was seen that pemetrexed decreased the levels of total 4E-BP1 as compared to control (Fig 20 B) but there was no dose-dependent effect apparent. However, the intensity of darkness shifted from more phosphorylated forms down to the less phosphorylated form with greater hypophosphorylation observed at highest pemetrexed concentration (640 nM) (Fig 20A). Unphosphorylated 4E-BP1 is known to tightly bind to eIF4E-capped mRNA complexes, preventing the binding of eIF4G and the initiation of cap-dependent translation, so we measured the binding of 4E-BP1 to eIF4E-cap complexes in extracts of drug-treated cells. The binding of 4E-BP1 to eIF4E-bound 7-methylGTP-beads was enhanced by pemetrexed and the hypophosphorylated form that was predominant at the highest concentration of pemetrexed (Fig. 20B), indicating that pemetrexed inhibited initiation of cap-dependent translation. Taken together, it was observed that pemetrexed was able to inhibit mTOR signaling as evident from inhibition of mTOR substrates S6K1 and 4E-BP1.

AZD8055 (lanes 6, 7, and 8; Figure 20A and 20B) was much more potent than pemetrexed at inhibition of the phosphorylation of S6K1 and of 4E-BP1 at fractional concentrations of its IC_{50}. AZD8055 demonstrated very high potency at hypophosphorylating both the substrates even at 0.5X IC_{50} with a tremendous inhibitory effect at higher concentrations. The levels of total 4E-BP1 were dose-dependently reduced with the hypophosphorylated form predominant at higher concentrations (Figure 20A and 20B). On assessing the levels of 4E-BP1–eIF4E-7mGTP-bound capped complexes, a significant enhancement was seen with AZD8055 treatment which increased in intensity with increase in dose of AZD8055. It suggested that AZD8055 was more efficient than pemetrexed in inhibiting mTOR kinase.

When pemetrexed at an IC_{50} concentration was combined with fractional IC_{50} concentrations of AZD8055 (lanes 9, 10, and 11; Figure 20A and 20B), the phosphoryaltion of S6K1 was substantially lower as compared to untreated and pemetrexed IC_{50}-treated cells, but the effect was not consistent over graded IC_{50} concentrations of AZD8055. Similarly, phosphorylation of 4E-BP1 by a combinaiton of AZD8055 and PTX was decreased compared to control and pemetrexed alone at their IC_{50}s. However, addition of pemetrexed IC_{50} to fractional IC_{50}s of AZD8055 did not have any benefit over the individual fractional IC_{50}s of AZD8055 in inhibiting phosphorylation of 4E-BP1. If any, there was increase in phosphorylation seen in lanes 10 and 11 compared to lanes 7 and 8. Total 4E-BP1 levels were decreased compared to untreated cells, but no significant difference was observed over lane 4 and lanes 6, 7, and 8. However, there was an apparent increase in hypophosphorylated form in lane 11 over lane 4 and lane 8 suggested that phosphorylation was decreased with the combination. The 4E-BP1–eIF4E-7mGTP-bound capped complex levels showed a decrease initially (compare lane 9 and lane 10) but it gradually increased with increase in dose (compare lane 10 and 11). This data indicated that addition of IC_{50} dose of pemetrexed to AZD8055 did not have any major benefit over AZD8055 as a single agent on inhibition of mTORC1.

On the other hand, when IC_{50} dose of AZD8055 was added to fractional IC_{50}s of pemetrexed (lanes 12, 13, and 14), phosphorylation of S6K1 was inhibited much greater than with either drug alone. On the

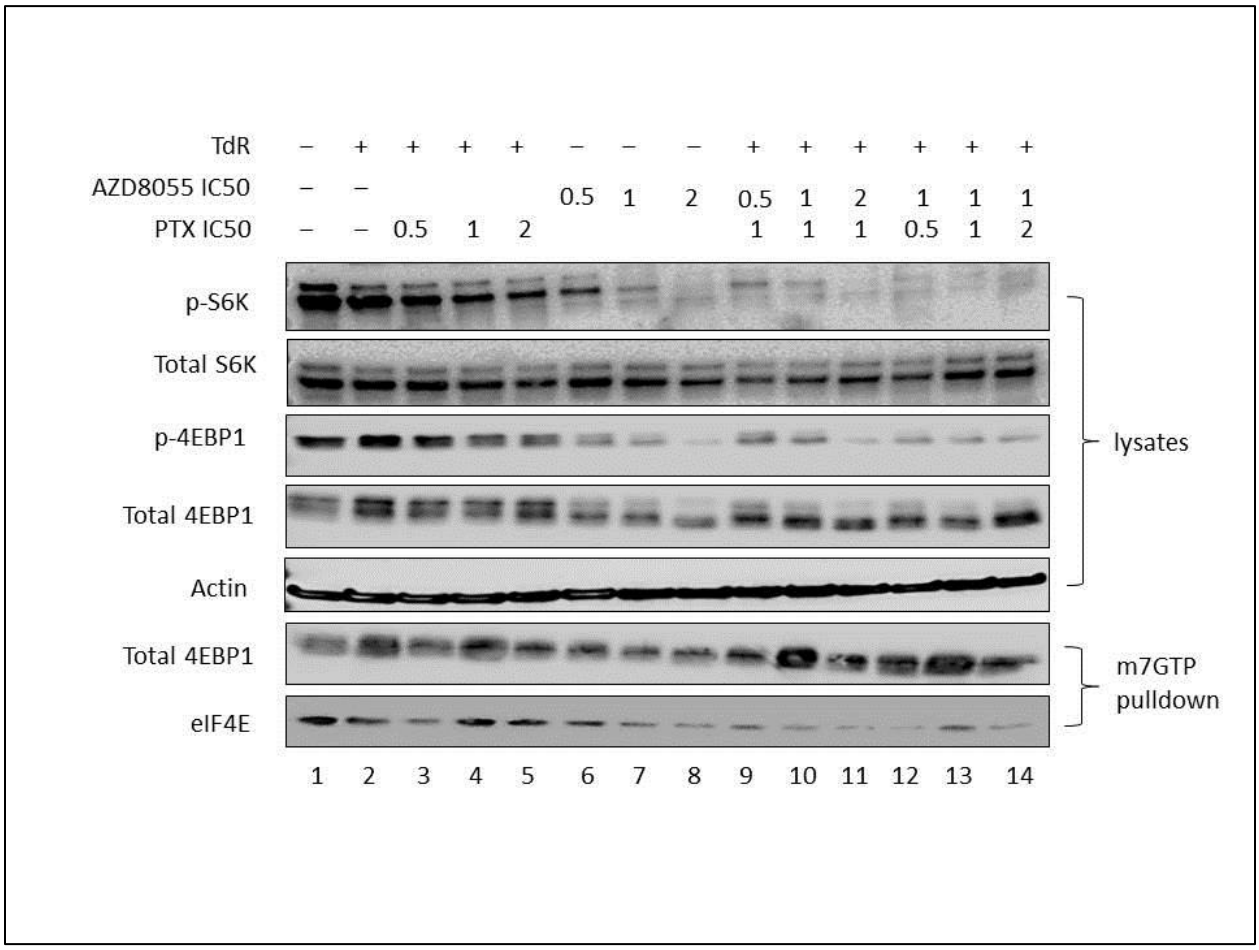

Figure 20 A: mTOR signaling events following treatments with pemetrexed (+ thymidine) and AZD8055, experiment 1.

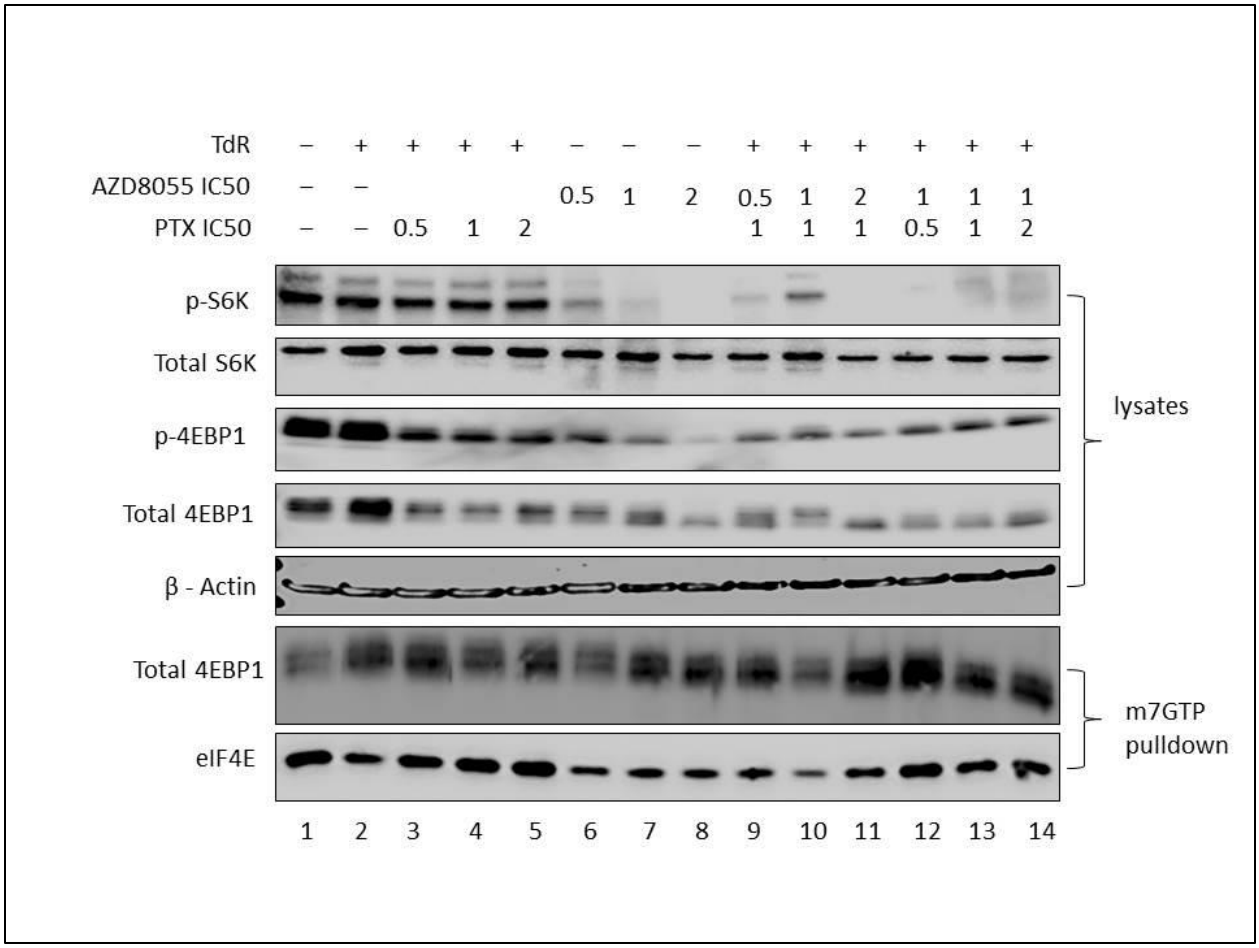

Figure 20 B: mTOR signaling events following treatments with pemetrexed (+ thymidine) and AZD8055, experiment 2.

contrary, though phopho-4E-BP1 levels were lower with concentrations of both drugs than seen at equivalent pemetrexed fractional IC_{50}s (compare lanes 12, 13 and 14 to lanes 3, 4, and 5 respectively), they were increased when compared to AZD8055 IC_{50}s (compare lanes 12, 13 and 14 to lane 7). Total 4E-BP1 levels showed a decrease with the combination over individual drugs with the unphosphorylated form predominant. The 4E-BP1–eIF4E-7mGTP-bound capped complex levels demonstrated highest levels with the combination of drugs.

Taken together, we concluded that pemetrexed ad AZD8055 exhibited inhibition of mTOR as individual drugs, but this inhibtion was greater with the combination of these two drugs. However, it looks like much of the inhibitory effects of the combination on mTORC1 are mediated by AZD8055 and pemetrexed does not add much to the combination with regards to inhibtion of mTORC1. The ability of AZD8055 to completely inhibit mTOR at both the complexes might explain this potency of AZD8055.

3.8 Effects of combining pemetrexed and AZD8055, in the absence of thymidine

In order to study the effects of pemetrexed in clinically relevant conditions, the aforementioned experiment was conducted in the absence of thymidine (Figure 21). AZD8055 was used at the concentrations mentioned in section 3.5. For pemetrexed, in the absence of thymidine, it is more potent and exhibts an IC_{50} in the range of 40 – 50 nM. Hence the concentrations used for pemetrexed were 25, 50 and 100 nM. It was seen that, with these concentrations which were more than 5-fold lower than those used in the presence of thymidine, pemetrexed (lanes 2, 3, and 4) inhibited phosphorylation of S6K1 much more. Unlike the experiment using PTX and thymidine, levels of total S6K1 were greatly inhibited by these concentrations of pemetrexed. It was also apparent that phosphorylation of 4E-BP1 and levels of total 4E-BP1 were significantly reduced under pemetrexed treatment and the reduction was dose-dependent. As observed with this combination in the presence of thymidine, the 4E-BP1 bands shifted towards the hypophosphorylated form at 100 nM pemetrexed, indicating that phosphorylation was

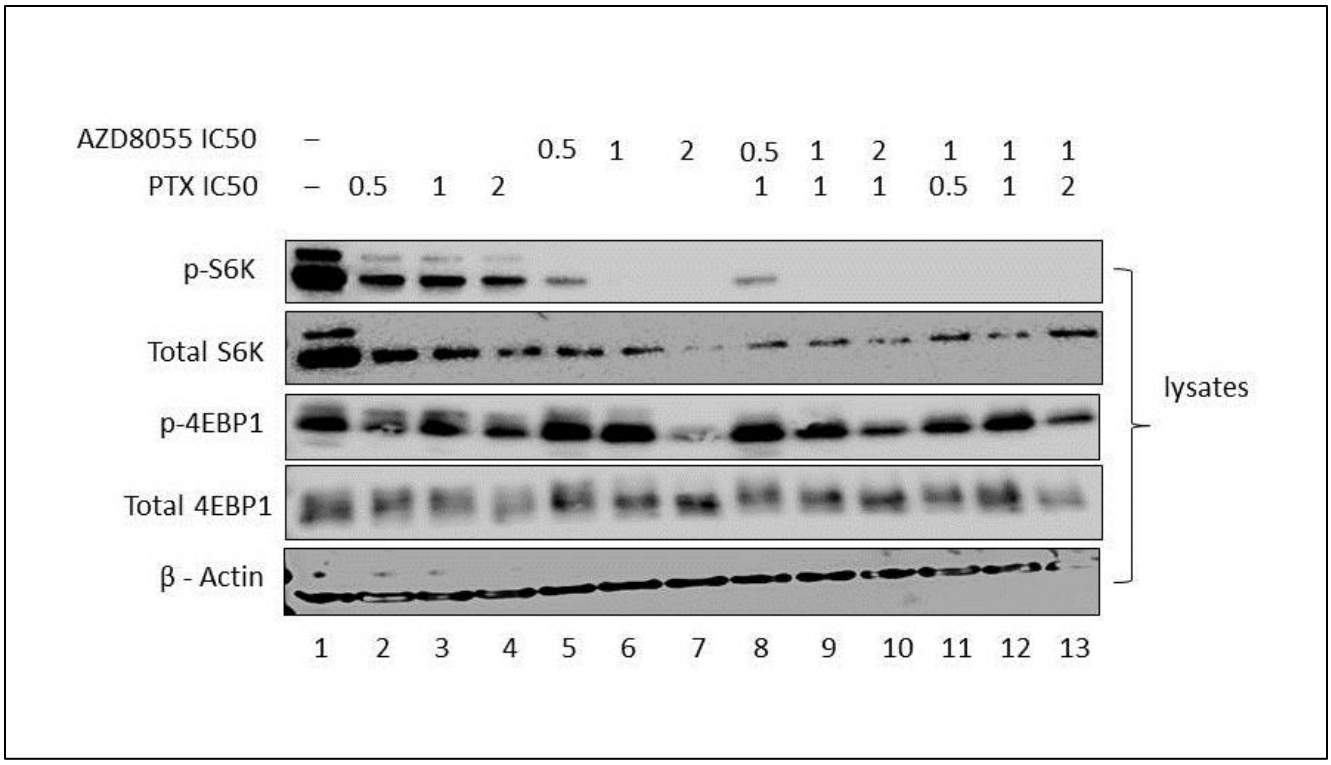

Figure 21: mTOR signaling events following treatments with pemetrexed and AZD8055, in the absence of thymidine.

reduced. AZD8055 (lanes 5, 6, and 7) demonstrated dose-dependent decrease in the levels of phopho and total S6K1; while p-4E-BP1 levels increased with 0.5 and 1X IC_{50} of AZD8055 (lanes 5 and 6; p-4E-BP1), they decreased with further increment in dose. Total 4E-BP1 showed a dose-dependent decrease with a predominance of the hypophosphorylated form at increasing AZD8055, suggesting that phosphorylation was inhibited. The addition of IC_{50} concentrations of pemetrexed to fractional IC_{50} concentrations of AZD8055 (lanes 8, 9, and 10) did not show any superior effects over fractional IC50s of AZD8055 alone (compare lanes 8, 9, and 10 to lanes 5, 6, and 7). But, when IC_{50} of AZD8055 was added to fractional IC_{50}s of pemetrexed (lanes 11, 12, and 13), the effects on phosphorylation events of both S6K1 and 4e-bp1 was significantly higher with pemetrexed alone (compare lanes 11, 12, and 13 to lanes 2, 3, and 4). The difference in levels of total S6K1 was apparent also, but no difference was observed for total 4E-BP1 levels. From this experiment, it was evident that pemetrexed in the absence of thymidine was much more potent as an inhibitor of mTORC1 than in the presence of thymidine, with low nanomolar concentrations sufficient to inhibit mTORC1 kinase activity. AZD8055 was always superior to pemetrexed in inhibiting mTOR function. The combination treatments did not show any significant differences from AZD8055 as a single drug, but they were different from pemetrexed as a single drug. It can be concluded that most of the effects of the combination treatment on mTORC1 activity were mediated via AZD8055 in the absence of thymidine similar to what was seen in thymidine-containing medium.

Chapter 4: Discussion

Adenosine monophosphate (AMP)-activated protein kinase (AMPK) acts as a sensor of energy status and modulates cellular functions that drive cell growth and proliferation. mTOR is the target of rapamycin which was initially discovered as a macrolide antibiotic but gained attention because of its antiproliferative properties. mTOR regulates protein synthesis via S6K1 and 4E-BP1, and dysregulation of mTOR signaling is seen in most cancers. It has been shown that activated AMPK directly inhibits mTORC1 kinase endogenously by TSC2 and raptor phosphorylation (Gwinn et al. 2008, Inoki et al. 2003). mTOR, an integral protein of the mTOR signaling pathway responds to intracellular and extracellular signals to serve as a central regulator of cell metabolism, growth, proliferation and survival. Alterations in these pathways can contribute to human disease states, including cancer (Calkhoven et al. 2002). AMPK is activated by the antidiabetic drug metformin (Hardie 2011), and it was observed that diabetics on metformin therapy had lower incidence of cancer than those on other anti-diabetic agents (Lin et al. 2014). Thus, it was evident that regulation of AMPK and mTOR are of importance with respect to cell survival and metabolism, and alterations in this pathway could predispose organisms to cancer. The purpose of this dissertation was to determine the interactions of activation of AMPK and direct pharmacological inhibition of mTOR and how the combined effect suppresses NSCLC cell proliferation.

AICAR is a classical activator of AMPK. It gets converted to ZMP and mimics AMP to activate AMPK (Hardie 2011). Pemetrexed is an antifolate used for the treatment of NSCLC. Recently, our laboratory reported that pemetrexed, in addition to inhibition of TS, inhibited a second folate-dependent enzyme of de novo purine synthesis, AICART, leading to AMPK activation and subsequent mTORC1 inhibition. To address our hypothesis, we combined the activators of AMPK, AICAR and/or pemetrexed, with dual mTORC1/2 inhibitor AZD8055 to determine the combined effects on cell growth and proliferation. Rapamycin and its analogs are strong inhibitors of mTORC1; hence we evaluated the efficacy of a rapamycin analog RAD001 on H661, H441, and H358 cell lines. Growth suppression experiments with

RAD001 and AZD8055 revealed dramatic differences in efficacy of the compounds. It was observed that the ATP-site mTOR inhibitor AZD8055 demonstrated stronger growth suppression effects than the rapalog, RAD001 (Figure 11 and Figure 12). Due to the excellent growth inhibitory effects observed with AZD8055, we concentrated on combining AZD8055 with the AMPK activating drug pemetrexed. The effects of pemetrexed are altered by the presence or absence of thymidine. In the former case, pemetrexed effects are only directed towards inhibition of AICART and activation of AMPK. Addition of thymidine to the media provides a salvageable source of thymidine which prevents the cellular effects of TS inhibition by pemetrexed. In the latter, pemetrexed acts as an inhibitor of both AICART and TS and is more potent. When AZD8055 was combined with pemetrexed in the presence of thymidine, a striking synergism was observed in suppression of growth of H358 cells (Figure 16). This led to the hypothesis that activation of AMPK would enhance direct pharmacological inhibition of mTORC1. Surprisingly, when this hypothesis was tested using a classical activator of AMPK, AICAR, the drug interaction was found to be additive (Figure 14) implying that growth limiting effects of pemetrexed in the presence of thymidine appear to be more complex than just activation of AMPK and subsequent inhibition of mTORC1 signaling.

The effects of combination of pemetrexed and AZD8055 on mTORC1 signaling were directly studied by immunoblotting. We observed that AZD8055 and pemetrexed, in the presence or absence of thymidine, each inhibited mTORC1 signaling as single agents evident by hypophosphorylations of mTORC1 substrates S6K1 and 4E-BP1. It was clear that both, pemetrexed (+ thymidine) and AZD8055, and pemetrexed (- thymidine) and AZD8055 inhibited mTORC1 signaling events. This is of great importance clinically as pemetrexed without thymidine is the clinically relevant condition and under these conditions, pemetrexed in combination with AZD8055 showed excellent anti-proliferative effects. Additionally, AZD8055 demonstrated superior effects over pemetrexed in inhibiting phosphorylation of S6K1 and 4E-BP1 implying that AZD8055 was more potent on mTORC1 inhibition than pemetrexed. This was interesting because the concentrations of both the drugs chosen were the same fractions of IC_{50} and

therefore, we were testing whether the effects on mTORC1 signaling were responsible for inhibiting growth of cells at the first active concentrations of drugs. From this analysis, it was clear that given the intensity of mTOR signaling inhibition when an IC_{50} concentration of AZD8055 was combined with fractional IC_{50}s of pemetrexed, AZD8055 inhibited mTORC1 signaling to a greater level than pemetrexed. We reached a conclusion that although AMPK activation in mTORC1 inhibition were involved in the effects of pemetrexed, other effects of this drug might well be involved in the most sensitive steps that lead to growth inhibition. This idea needs further investigation.

During the course of this dissertation, several interesting observations were made whose basis was not evident. It was seen that the combination of pemetrexed and AZD8055, in the presence of thymidine exhibited prominent synergism, while in the absence of thymidine; the interaction of pemetrexed with AZD8055 demonstrated a much lower level of synergism and was nearly additive. Pemetrexed in the absence of thymidine is more potent than in the presence of thymidine, demonstrating more than a 6-fold lower IC_{50} concentration in H358 cells. Another notable observation was that pemetrexed in the absence of thymidine greatly inhibited phosphorylation of S6K1 and 4E-BP1 compared to that in the presence of thymidine. Moreover, it was also able to reduce the levels of total S6K1 and 4E-BP1 compared to that in the presence of thymidine. This was interesting because immunoblotting was performed at fractional IC_{50} concentrations treatment meaning pemetrexed in the absence of thymidine was used at 6-fold lower concentrations than that in the presence of thymidine but showed greater inhibitory effects on mTORC1 signaling. It was not clear why this was observed; however, it appears that pemetrexed activity on mTORC1 might involve other unknown mechanisms.

Pemetrexed is an US FDA approved drug for the first-line treatment of NSCLC in combination with cisplatin (Scagliotti et al. 2008). Interestingly, we observed that the H441 and H358 cell lines which have mutations in the KRAS gene showed greater sensitivity to pemetrexed than the H661cell line in which KRAS was wild type. Recently, a study from another laboratory (Moran et al. 2014) has shown that NSCLC cell lines with mutant KRAS gene were measurably more sensitive to PTX than NSCLC lines

with wild type KRAS. They reported that KRAS-mutant NSCLC cell lines showed greater dependency on folate metabolism pathways compared with KRAS wild-type NSCLC cell lines. They also reported that, following antifolate treatment, there was a robust downregulation of KRAS mRNA expression in both KRAS-mutant and wild-type cells and total KRAS protein expression and KRAS activity were decreased in KRAS-mutant cells (Moran et al. 2014). This was consistent with our observation that differential sensitivity to pemetrexed was observed with H441 and H358, and H661 (Figure 13). This is very important in NSCLC chemotherapy as KRAS is one of the most frequently mutated genes in lung carcinomas (Ding et al. 2008). Furthermore, it was interesting to note that H661 cell line which was least sensitive to pemetrexed has a mutation in the p16 gene. p16 is a tumor suppressor gene important in cell cycle regulation. The pl6 protein inhibits CDK4/6 and thereby prevents phosphorylation of Rb and cell cycle progression. It has been shown that pl6 and Rb are members of a growth-regulatory pathway often inactivated during tumor progression. (Stone et al. 1995). This could be one of the other reasons for H661 not being very sensitive to pemetrexed.

This study tested a novel hypothesis of combining dual mTORC1/2 inhibitor AZD8055 with an AMPK activator pemetrexed. A recent study by Kawabata et al. (2014) showed that the combination of rapamycin and pemetrexed exhibited synergistic interaction on growth suppression of NSCLC cells with enhancement of mTOR inhibition. They also reported that rapamycin leads to a weak downregulation of endogenous expression of TS that they interpreted to confer increased response to pemetrexed (Kawabata et al. 2014). In that study, it also was important to note the mutational status of the NSCLC cell lines. The NSCLC cell lines that showed sensitivity to the combination of rapamycin and pemetrexed harbored mutations in the PIK3CA or PTEN genes. When the same study was conducted in NSCLC cells lacking these mutations, rapamycin did not enhance the efficacy of pemetrexed in these cell lines (Kawabata et al. 2014). This was consistent with our findings that the rapamycin analog RAD001 (everolimus) did not exhibit strong potency in inhibiting the proliferation of H661, H441, and H358. None of these cell lines have mutations in the PIK3CA or PTEN genes. Additionally, Markova et al. (2011) have shown that

rapalogs may suppress the anti-tumor activity of pemetrexed by slowing cell cycle progression. Our results have revealed that combining a dual mTORC1/2 inhibitor AZD8055 with pemetrexed has a synergistic to near additive interaction on inhibition of proliferation of NSCLC cells and these effects are mediated by inhibition mTORC1 signaling. However, other effects of pemetrexed might play an important role in controlling cell growth and more studies are needed to examine this mechanism.

Future studies should be directed towards understanding the mechanisms of cell kill by the combination of pemetrexed and AZD8055. It would be a good approach to evaluate the effects of this combination on basal levels of TS. Given that AZD8055 markedly inhibits mTORC1 signaling at lower concentrations, studies are needed to evaluate the effects of AZD8055 on mTORC2 substrate Akt and subsequent feedback on mTORC1. It has been shown that inhibition of mTOR kinase by AZD8055 relieves inhibition of receptor tyrosine kinases (RTK) via the IRS-1 feedback loop, leading to subsequent PI3K activation and rephosphorylation of Akt T308 sufficient to reactivate Akt activity and mTORC1 signaling (Rodrik-Outmezguine et al. 2011). Thus, effects of combining AZD8055 with RTK inhibitor Sorafenib should be considered.

Collectively, our studies have revealed that the combination of pemetrexed and AZD8055 has a synergistic to near additive effect on growth suppression of NSCLC cells; these effects appear to be mediated via mTORC1 signaling. mTORC1 inhibition is more pronounced with AZD8055 suggesting that additional mechanisms of cell kill would exist with pemetrexed treatment that needs further investigation.

Literature Cited

ALI, A. and BHATTACHARYA, S., 2014. DNA binders in clinical trials and chemotherapy. *Bioorganic & medicinal chemistry,* .

ANDRADE-VIEIRA, R., XU, Z., COLP, P. and MARIGNANI, P.A., 2013. Loss of LKB1 expression reduces the latency of ErbB2-mediated mammary gland tumorigenesis, promoting changes in metabolic pathways. *PloS one,* **8**(2), pp. e56567.

BRAMBILLA, E., TRAVIS, W.D., COLBY, T.V., CORRIN, B. and SHIMOSATO, Y., 2001. The new World Health Organization classification of lung tumours. *The European respiratory journal,* **18**(6), pp. 1059-1068.

CALKHOVEN, C.F., MULLER, C. and LEUTZ, A., 2002. Translational control of gene expression and disease. *Trends in molecular medicine,* **8**(12), pp. 577-583.

CHOU, T.C., 2010. Drug combination studies and their synergy quantification using the Chou-Talalay method. *Cancer research,* **70**(2), pp. 440-446.

CHRESTA, C.M., DAVIES, B.R., HICKSON, I., HARDING, T., COSULICH, S., CRITCHLOW, S.E., VINCENT, J.P., ELLSTON, R., JONES, D., SINI, P., JAMES, D., HOWARD, Z., DUDLEY, P., HUGHES, G., SMITH, L., MAGUIRE, S., HUMMERSONE, M., MALAGU, K., MENEAR, K., JENKINS, R., JACOBSEN, M., SMITH, G.C., GUICHARD, S. and PASS, M., 2010. AZD8055 is a potent, selective, and orally bioavailable ATP-competitive mammalian target of rapamycin kinase inhibitor with in vitro and in vivo antitumor activity. *Cancer research,* **70**(1), pp. 288-298.

D'ARCANGELO, M., D'INCECCO, A. and CAPPUZZO, F., 2013. Rare mutations in non-small-cell lung cancer. *Future oncology (London, England),* **9**(5), pp. 699-711.

DING, L., GETZ, G., WHEELER, D.A., MARDIS, E.R., MCLELLAN, M.D., CIBULSKIS, K., SOUGNEZ, C., GREULICH, H., MUZNY, D.M., MORGAN, M.B., FULTON, L., FULTON, R.S., ZHANG, Q., WENDL, M.C., LAWRENCE, M.S., LARSON, D.E., CHEN, K., DOOLING, D.J., SABO, A., HAWES, A.C., SHEN, H., JHANGIANI, S.N., LEWIS, L.R., HALL, O., ZHU, Y., MATHEW, T., REN, Y., YAO, J., SCHERER, S.E., CLERC, K., METCALF, G.A., NG, B., MILOSAVLJEVIC, A., GONZALEZ-GARAY, M.L., OSBORNE, J.R., MEYER, R., SHI, X., TANG, Y., KOBOLDT, D.C., LIN, L., ABBOTT, R., MINER, T.L., POHL, C., FEWELL, G., HAIPEK, C., SCHMIDT, H., DUNFORD-SHORE, B.H., KRAJA, A., CROSBY, S.D., SAWYER, C.S., VICKERY, T., SANDER, S., ROBINSON, J., WINCKLER, W., BALDWIN, J., CHIRIEAC, L.R., DUTT, A., FENNELL, T., HANNA, M., JOHNSON, B.E., ONOFRIO, R.C., THOMAS, R.K., TONON, G., WEIR, B.A., ZHAO, X., ZIAUGRA, L., ZODY, M.C., GIORDANO, T., ORRINGER, M.B., ROTH, J.A., SPITZ, M.R., WISTUBA, I.I., OZENBERGER, B., GOOD, P.J., CHANG, A.C., BEER, D.G., WATSON, M.A., LADANYI, M., BRODERICK, S., YOSHIZAWA, A., TRAVIS, W.D., PAO, W., PROVINCE, M.A., WEINSTOCK, G.M., VARMUS, H.E., GABRIEL, S.B., LANDER, E.S., GIBBS, R.A., MEYERSON, M. and WILSON, R.K., 2008. Somatic mutations affect key pathways in lung adenocarcinoma. *Nature,* **455**(7216), pp. 1069-1075.

ETTINGER, D.S., AKERLEY, W., BORGHAEI, H., CHANG, A.C., CHENEY, R.T., CHIRIEAC, L.R., D'AMICO, T.A., DEMMY, T.L., GANTI, A.K., GOVINDAN, R., GRANNIS, F.W.,Jr,

HORN, L., JAHAN, T.M., JAHANZEB, M., KESSINGER, A., KOMAKI, R., KONG, F.M., KRIS, M.G., KRUG, L.M., LENNES, I.T., LOO, B.W.,Jr, MARTINS, R., O'MALLEY, J., OSAROGIAGBON, R.U., OTTERSON, G.A., PATEL, J.D., PINDER-SCHENCK, M.C., PISTERS, K.M., RECKAMP, K., RIELY, G.J., ROHREN, E., SWANSON, S.J., WOOD, D.E., YANG, S.C., HUGHES, M., GREGORY, K.M. and NCCN (NATIONAL COMPREHENSIVE CANCER NETWORK), 2012. Non-small cell lung cancer. *Journal of the National Comprehensive Cancer Network : JNCCN,* **10**(10), pp. 1236-1271.

FELDMAN, M.E., APSEL, B., UOTILA, A., LOEWITH, R., KNIGHT, Z.A., RUGGERO, D. and SHOKAT, K.M., 2009. Active-site inhibitors of mTOR target rapamycin-resistant outputs of mTORC1 and mTORC2. *PLoS biology,* **7**(2), pp. e38.

FUMAROLA, C., BONELLI, M.A., PETRONINI, P.G. and ALFIERI, R.R., 2014. Targeting PI3K/AKT/mTOR pathway in non small cell lung cancer. *Biochemical pharmacology,* .

GROENEWOUD, M.J. and ZWARTKRUIS, F.J., 2013. Rheb and Rags come together at the lysosome to activate mTORC1. *Biochemical Society transactions,* **41**(4), pp. 951-955.

GUERTIN, D.A. and SABATINI, D.M., 2009. The pharmacology of mTOR inhibition. *Science signaling,* **2**(67), pp. pe24.

GUERTIN, D.A., STEVENS, D.M., THOREEN, C.C., BURDS, A.A., KALAANY, N.Y., MOFFAT, J., BROWN, M., FITZGERALD, K.J. and SABATINI, D.M., 2006. Ablation in mice of the mTORC components raptor, rictor, or mLST8 reveals that mTORC2 is required for signaling to Akt-FOXO and PKCalpha, but not S6K1. *Developmental cell,* **11**(6), pp. 859-871.

GWINN, D.M., SHACKELFORD, D.B., EGAN, D.F., MIHAYLOVA, M.M., MERY, A., VASQUEZ, D.S., TURK, B.E. and SHAW, R.J., 2008. AMPK phosphorylation of raptor mediates a metabolic checkpoint. *Molecular cell,* **30**(2), pp. 214-226.

HAN, D., LI, S.J., ZHU, Y.T., LIU, L. and LI, M.X., 2013. LKB1/AMPK/mTOR signaling pathway in non-small-cell lung cancer. *Asian Pacific journal of cancer prevention : APJCP,* **14**(7), pp. 4033-4039.

HARA, K., MARUKI, Y., LONG, X., YOSHINO, K., OSHIRO, N., HIDAYAT, S., TOKUNAGA, C., AVRUCH, J. and YONEZAWA, K., 2002. Raptor, a binding partner of target of rapamycin (TOR), mediates TOR action. *Cell,* **110**(2), pp. 177-189.

HARDIE, D.G., 2011. Adenosine monophosphate-activated protein kinase: a central regulator of metabolism with roles in diabetes, cancer, and viral infection. *Cold Spring Harbor symposia on quantitative biology,* **76**, pp. 155-164.

HARDIE, D.G., 2011. AMP-activated protein kinase: an energy sensor that regulates all aspects of cell function. *Genes & development,* **25**(18), pp. 1895-1908.

HARDIE, D.G., 2011. AMP-activated protein kinase: an energy sensor that regulates all aspects of cell function. *Genes & development,* **25**(18), pp. 1895-1908.

HEAVEY, S., O'BYRNE, K.J. and GATELY, K., 2014. Strategies for co-targeting the PI3K/AKT/mTOR pathway in NSCLC. *Cancer treatment reviews,* **40**(3), pp. 445-456.

HOUGHTON, P.J., 2010. Everolimus. *Clinical cancer research : an official journal of the American Association for Cancer Research,* **16**(5), pp. 1368-1372.

HOYER-HANSEN, M. and JAATTELA, M., 2007. AMP-activated protein kinase: a universal regulator of autophagy? *Autophagy,* **3**(4), pp. 381-383.

HSIEH, A.C., LIU, Y., EDLIND, M.P., INGOLIA, N.T., JANES, M.R., SHER, A., SHI, E.Y., STUMPF, C.R., CHRISTENSEN, C., BONHAM, M.J., WANG, S., REN, P., MARTIN, M., JESSEN, K., FELDMAN, M.E., WEISSMAN, J.S., SHOKAT, K.M., ROMMEL, C. and RUGGERO, D., 2012. The translational landscape of mTOR signalling steers cancer initiation and metastasis. *Nature,* **485**(7396), pp. 55-61.

JONES, R.G., PLAS, D.R., KUBEK, S., BUZZAI, M., MU, J., XU, Y., BIRNBAUM, M.J. and THOMPSON, C.B., 2005. AMP-activated protein kinase induces a p53-dependent metabolic checkpoint. *Molecular cell,* **18**(3), pp. 283-293.

KAIZUKA, T., HARA, T., OSHIRO, N., KIKKAWA, U., YONEZAWA, K., TAKEHANA, K., IEMURA, S., NATSUME, T. and MIZUSHIMA, N., 2010. Tti1 and Tel2 are critical factors in mammalian target of rapamycin complex assembly. *The Journal of biological chemistry,* **285**(26), pp. 20109-20116.

KAWABATA, S., CHIANG, C.T., TSURUTANI, J., SHIGA, H., ARWOOD, M.L., KOMIYA, T., GILLS, J.J., MEMMOTT, R.M. and DENNIS, P.A., 2014. Rapamycin downregulates thymidylate synthase and potentiates the activity of pemetrexed in non-small cell lung cancer. *Oncotarget,* **5**(4), pp. 1062-1070.

KIM, D.H., SARBASSOV, D.D., ALI, S.M., KING, J.E., LATEK, R.R., ERDJUMENT-BROMAGE, H., TEMPST, P. and SABATINI, D.M., 2002. mTOR interacts with raptor to form a nutrient-sensitive complex that signals to the cell growth machinery. *Cell,* **110**(2), pp. 163-175.

KURTH-KRACZEK, E.J., HIRSHMAN, M.F., GOODYEAR, L.J. and WINDER, W.W., 1999. 5' AMP-activated protein kinase activation causes GLUT4 translocation in skeletal muscle. *Diabetes,* **48**(8), pp. 1667-1671.

LAPLANTE, M. and SABATINI, D.M., 2012. mTOR signaling in growth control and disease. *Cell,* **149**(2), pp. 274-293.

LAPLANTE, M. and SABATINI, D.M., 2009. mTOR signaling at a glance. *Journal of cell science,* **122**(Pt 20), pp. 3589-3594.

LIN, J.T., CHEN, H.M., CHIU, C.H. and LIANG, Y.J., 2014. AMP-activated protein kinase activators in diabetic ulcers: from animal studies to Phase II drugs under investigation. *Expert opinion on investigational drugs,* , pp. 1-13.

LIU, Q., THOREEN, C., WANG, J., SABATINI, D. and GRAY, N.S., 2009. mTOR Mediated Anti-Cancer Drug Discovery. *Drug discovery today.Therapeutic strategies,* **6**(2), pp. 47-55.

MA, X.M. and BLENIS, J., 2009. Molecular mechanisms of mTOR-mediated translational control. *Nature reviews.Molecular cell biology,* **10**(5), pp. 307-318.

MANNING, B.D., 2004. Balancing Akt with S6K: implications for both metabolic diseases and tumorigenesis. *The Journal of cell biology,* **167**(3), pp. 399-403.

MARTINEZ, M.E., MARSHALL, J.R. and GIOVANNUCCI, E., 2008. Diet and cancer prevention: the roles of observation and experimentation. *Nature reviews.Cancer,* **8**(9), pp. 694-703.

MARTINI, M., DE SANTIS, M.C., BRACCINI, L., GULLUNI, F. and HIRSCH, E., 2014. PI3K/AKT signaling pathway and cancer: an updated review. *Annals of Medicine,* , pp. 1-12.

MERIC-BERNSTAM, F. and GONZALEZ-ANGULO, A.M., 2009. Targeting the mTOR signaling network for cancer therapy. *Journal of clinical oncology : official journal of the American Society of Clinical Oncology,* **27**(13), pp. 2278-2287.

MORAN, D.M., TRUSK, P.B., PRY, K., PAZ, K., SIDRANSKY, D. and BACUS, S.S., 2014. KRAS Mutation Status Is Associated with Enhanced Dependency on Folate Metabolism Pathways in Non-Small Cell Lung Cancer Cells. *Molecular cancer therapeutics,* **13**(6), pp. 1611-1624.

O'REILLY, K.E., ROJO, F., SHE, Q.B., SOLIT, D., MILLS, G.B., SMITH, D., LANE, H., HOFMANN, F., HICKLIN, D.J., LUDWIG, D.L., BASELGA, J. and ROSEN, N., 2006. mTOR inhibition induces upstream receptor tyrosine kinase signaling and activates Akt. *Cancer research,* **66**(3), pp. 1500-1508.

OWONIKOKO, T.K., RAMALINGAM, S.S. and BELANI, C.P., 2010. Maintenance therapy for advanced non-small cell lung cancer: current status, controversies, and emerging consensus. *Clinical cancer research : an official journal of the American Association for Cancer Research,* **16**(9), pp. 2496-2504.

PETERS, S., ADJEI, A.A., GRIDELLI, C., RECK, M., KERR, K., FELIP, E. and ESMO GUIDELINES WORKING GROUP, 2012. Metastatic non-small-cell lung cancer (NSCLC): ESMO Clinical Practice Guidelines for diagnosis, treatment and follow-up. *Annals of Oncology : Official Journal of the European Society for Medical Oncology / ESMO,* **23 Suppl 7**, pp. vii56-64.

PETERSON, T.R., LAPLANTE, M., THOREEN, C.C., SANCAK, Y., KANG, S.A., KUEHL, W.M., GRAY, N.S. and SABATINI, D.M., 2009. DEPTOR is an mTOR inhibitor frequently overexpressed in multiple myeloma cells and required for their survival. *Cell,* **137**(5), pp. 873-886.

RACANELLI, A.C., ROTHBART, S.B., HEYER, C.L. and MORAN, R.G., 2009. Therapeutics by cytotoxic metabolite accumulation: pemetrexed causes ZMP accumulation, AMPK activation, and mammalian target of rapamycin inhibition. *Cancer research,* **69**(13), pp. 5467-5474.

RODRIK-OUTMEZGUINE, V.S., CHANDARLAPATY, S., PAGANO, N.C., POULIKAKOS, P.I., SCALTRITI, M., MOSKATEL, E., BASELGA, J., GUICHARD, S. and ROSEN, N., 2011. mTOR

kinase inhibition causes feedback-dependent biphasic regulation of AKT signaling. *Cancer discovery,* **1**(3), pp. 248-259.

ROTHBART, S.B., RACANELLI, A.C. and MORAN, R.G., 2010. Pemetrexed indirectly activates the metabolic kinase AMPK in human carcinomas. *Cancer research,* **70**(24), pp. 10299-10309.

SADLER, T.M., GAVRIIL, M., ANNABLE, T., FROST, P., GREENBERGER, L.M. and ZHANG, Y., 2006. Combination therapy for treating breast cancer using antiestrogen, ERA-923, and the mammalian target of rapamycin inhibitor, temsirolimus. *Endocrine-related cancer,* **13**(3), pp. 863-873.

SANCHEZ-CESPEDES, M., PARRELLA, P., ESTELLER, M., NOMOTO, S., TRINK, B., ENGLES, J.M., WESTRA, W.H., HERMAN, J.G. and SIDRANSKY, D., 2002. Inactivation of LKB1/STK11 is a common event in adenocarcinomas of the lung. *Cancer research,* **62**(13), pp. 3659-3662.

SCAGLIOTTI, G.V., PARIKH, P., VON PAWEL, J., BIESMA, B., VANSTEENKISTE, J., MANEGOLD, C., SERWATOWSKI, P., GATZEMEIER, U., DIGUMARTI, R., ZUKIN, M., LEE, J.S., MELLEMGAARD, A., PARK, K., PATIL, S., ROLSKI, J., GOKSEL, T., DE MARINIS, F., SIMMS, L., SUGARMAN, K.P. and GANDARA, D., 2008. Phase III study comparing cisplatin plus gemcitabine with cisplatin plus pemetrexed in chemotherapy-naive patients with advanced-stage non-small-cell lung cancer. *Journal of clinical oncology : official journal of the American Society of Clinical Oncology,* **26**(21), pp. 3543-3551.

SEHGAL, S.N., 2003. Sirolimus: its discovery, biological properties, and mechanism of action. *Transplantation proceedings,* **35**(3 Suppl), pp. 7S-14S.

SHACKELFORD, D.B. and SHAW, R.J., 2009. The LKB1-AMPK pathway: metabolism and growth control in tumour suppression. *Nature reviews.Cancer,* **9**(8), pp. 563-575.

SHAW, R.J., 2009. LKB1 and AMP-activated protein kinase control of mTOR signalling and growth. *Acta physiologica (Oxford, England),* **196**(1), pp. 65-80.

SHI, Y., YAN, H., FROST, P., GERA, J. and LICHTENSTEIN, A., 2005. Mammalian target of rapamycin inhibitors activate the AKT kinase in multiple myeloma cells by up-regulating the insulin-like growth factor receptor/insulin receptor substrate-1/phosphatidylinositol 3-kinase cascade. *Molecular cancer therapeutics,* **4**(10), pp. 1533-1540.

SHIMOBAYASHI, M. and HALL, M.N., 2014. Making new contacts: the mTOR network in metabolism and signalling crosstalk. *Nature reviews.Molecular cell biology,* **15**(3), pp. 155-162.

SIEGEL, R., NAISHADHAM, D. and JEMAL, A., 2013. Cancer statistics, 2013. *CA: a cancer journal for clinicians,* **63**(1), pp. 11-30.

STONE, S., JIANG, P., DAYANANTH, P., TAVTIGIAN, S.V., KATCHER, H., PARRY, D., PETERS, G. and KAMB, A., 1995. Complex structure and regulation of the P16 (MTS1) locus. *Cancer research,* **55**(14), pp. 2988-2994.

WAN, X., HARKAVY, B., SHEN, N., GROHAR, P. and HELMAN, L.J., 2007. Rapamycin induces feedback activation of Akt signaling through an IGF-1R-dependent mechanism. *Oncogene*, **26**(13), pp. 1932-1940.

WANG, L., HARRIS, T.E., ROTH, R.A. and LAWRENCE, J.C.,Jr, 2007. PRAS40 regulates mTORC1 kinase activity by functioning as a direct inhibitor of substrate binding. *The Journal of biological chemistry*, **282**(27), pp. 20036-20044.

WINKLER, G.C., BARLE, E.L., GALATI, G. and KLUWE, W.M., 2014. Functional differentiation of cytotoxic cancer drugs and targeted cancer therapeutics. *Regulatory toxicology and pharmacology : RTP*, .

ZHOU, C., WU, Y.L., CHEN, G., FENG, J., LIU, X.Q., WANG, C., ZHANG, S., WANG, J., ZHOU, S., REN, S., LU, S., ZHANG, L., HU, C., HU, C., LUO, Y., CHEN, L., YE, M., HUANG, J., ZHI, X., ZHANG, Y., XIU, Q., MA, J., ZHANG, L. and YOU, C., 2011. Erlotinib versus chemotherapy as first-line treatment for patients with advanced EGFR mutation-positive non-small-cell lung cancer (OPTIMAL, CTONG-0802): a multicentre, open-label, randomised, phase 3 study. *The lancet oncology*, **12**(8), pp. 735-742.

ZINZALLA, V., STRACKA, D., OPPLIGER, W. and HALL, M.N., 2011. Activation of mTORC2 by association with the ribosome. *Cell*, **144**(5), pp. 757-768.

Cancer.org

Weinberg, Robert. The biology of cancer, 2014.

VITA

Grinal Michael Corriea was born on July 26, 1988, in Mumbai, India, and is a citizen of India. She grew up in Vasai – a suburb of Mumbai. She completed her Bachelor of Pharmacy from University of Mumbai in 2010. Following that she worked with GlaxoSmithKline Pharmaceuticals as a Medical Representative and then, with Cegedim Strategic Data as a Market Research Analyst, both in Mumbai. She joined the master's program in the Department of Pharmacology and Toxicology at Virginia Commonwealth University (VCU), Richmond, Virginia in August 2012 and immediately entered the lab of Dr. Richard Moran and received her Master of Science in Pharmacology and Toxicology in 2014. She has been an active member of the Indian Student Organization at VCU, Tiranga and has served as the General Secretary for the academic year 2013-2014 and has been felicitated by the "Emerging Leader Award" by VCU in April 2014.